Experimental and model based investigation of the volumetric efficiency of a turbocharged natural gas engine

J.A.P.Willems

Delft University of Technology

TU Delft

Experimental and model based investigation of the volumetric efficiency of a turbocharged natural gas engine

by

J.A.P.Willems

to obtain the degree of Master of Science
at the Delft University of Technology,
to be defended publicly on Wednesday March 1, 2023 at 14:00.

Report number:	MT.22/23.025.M	
Student number:	4575393	
Thesis committee:	Dr. ir. P. de Vos,	TU Delft, Chairman
	Prof. dr. ir. R. van de Ketterij,	NLDA, Supervisor
	CDR. (ME) dr. ir. R. Geertsma,	NLDA & TU Delft
	Prof. dr. ir. B. J. Boersma,	TUDelft

An electronic version of this thesis is available at `http://repository.tudelft.nl/`.

TU Delft

Preface

I hereby present my master thesis ”Experimental and model based investigation of the volumetric efficiency of a turbocharged natural gas engine”. This is the last step in completing my master degree in marine technology with the specialisation marine engineering. Growing up near the harbor of Antwerp, seeing all the huge ships, I always had a passion for everything that happened on the water. My passion started with my first sailing lesson and led me to writing this master thesis.

I would like to thank the following people for guiding and supporting me in this process. First, I want to thank the Netherlands Defence Academy (NLDA) for providing me with an interesting thesis subject and great counselling. A special thanks to my supervisors at the NLDA; Rinze Geertsma and Robert van de Ketterij. They challenged me every week in this interesting subject and helped me bring this thesis to an academic level. Moreover, I want to thank Chris Dijkstra for his insights in new approaches he gave me. Also, I want to express my gratitude to the laboratory staff of the NLDA to guide me through the performed tests. Next, I want to thank Peter de Vos at the TUDelft for introducing me to the subject provided by the NLDA. I want to thank you not only for the introduction, but also for the feedback you gave me at the milestone meeting. It kept me on the wright track. Finally, I want to thank my friends and family to keep supporting me and giving me the encouragement I sometimes needed. A special thanks to my girlfriend who supported me the most.

J.A.P.Willems
Delft, February 2023

Abstract

As a big contributor to the the global emissions, the maritime sector strives to bring down its greenhouse gasses and hazardous emissions by enforcing increasing strict rules on the exhaust gasses. This gives major challenges to the maritime sector to develop greener modes of transportation.

This report investigates the in-cylinder starting conditions of spark ignited gas engines, as the starting conditions have a large influence on the efficiency and NOx emissions of gas engines. The investigation is based on experiments performed on a Caterpillar G3508 gas engine. These experiments gave an insight on the starting temperature, pressure and residual mass. With the acquired knowledge on the starting conditions, we improved the induction and volumetric efficiency prediction of a state of the art 0-dimensional engine model [15].

Another contribution of this paper is the development of a way to establish the volumetric efficiency from the amount of oxygen in the exhaust gas, for a natural gas engine. We used this method to check the improvements made to the engine model.

Out of the performed experiments, we concluded that the induced inlet mass temperature decreases with increasing power or mass flow. The insight found about the starting pressure for this engine is that the trapped pressure increases in relation to the manifold pressure with increasing power or mass flow. Together with an improved residual mass prediction, these insights resulted in an increase of the volumetric efficiency prediction accuracy by 2% at low powers and 10% at high power.

Contents

List of Figures

List of Tables

Nomenclature

Greek Symbols

α	crank angle	rad
χ_g	the ratio between the specific heats at constant pressure and air	
δ_f	fuel addition factor	-
ϵ	geometric compression ratio	-
ϵ_{inl}	Heat exchange effectiveness	-
η_{comb}	combustion efficiency	-
η_{fill}	filling efficiency	-
η_{TC}	turbocharger efficiency	-
η_v	volumetric efficiency	-
κ	specific heat ratio	-
λ	air excess ratio	-
λ_{CR}	crank rod ratio	-
ϕ	instantaneous crank angle	rad
π_{com}	compressor pressure ratio	-
π_{tur}	turbine pressure ratio	-
σ	stoichometric air to fuel ratio	-
τ	non-dimensional time or crank angle	-
ξ	reaction rate	kg/s

Roman Symbols

$\dot{m}$	mass flow	kg/s
$\dot{Q}$	heat rate	kJ/s
$\dot{W}$	work rate	kJ/s
a, b, c	seiliger parameters	-
A_B	Bore area	m^2
a_w	wiebe parameter	-
b_w	wiebe parameter	-
$c_{p,a}$	specific heat constant air at constant pressure	J/kgK
$c_{v,a}$	specific heat constant air at constant volume	J/kgK
D_B	Bore diameter	m

L_p	piston length	m
L_s	stroke length	m
L_{CR}	connecting rod length	m
M	molecular weight	????
m	mass	kg
m_w	wiebe shape factor	-
N	rotational speed	1/s
n	amount of mol	mol
n_c	polytropic compression exponent	-
n_e	polytropic expansion exponent	-
n_{bld}	polytropic exponent blowdown	m^2
n_{tc}	polytropic exponent of the turbine compression system	-
nr	amount of mol pr kg fuel	mol/kg
p	pressure	Pa
Q	Heat	kJ
q	specific heat release	kJ/kg
R	gas constant	J/kgK
r_c	effective compression ratio	-
r_v	effective expansion ratio	-
R_{CR}	crank radius	m
$r_{T,TC}$	driving temperature ratio of the turbocharger	-
T	temperature	K
t	time	s
U	internal energy	kJ
u_{comb}^{ref}	heat of formation at ref. temperature	kJ/kg
V	cylinder volume	m^3
V_s	stroke volume	m^2
w	specific work	kNm/kg
X	normalised combustion progression	-
x	mass fraction	-
y	mol fraction	-
Z	non-dimensional rate of combustion	-

subscripts

$1, 2, 3, 4, 5en6$	Seiliger stages

a	air
$actual$	actual
amb	ambient
b	burned
$comp$	compressor
d	exhaust receiver
da	dry air
dg	dry exhaust gas
em	exhaust manifold
ex	exhaust
f	fuel
g	exhaust gas
i	in
ic	intercooler
im	inlet mixture
$iman$	inlet manifold
ind	induction
$initial$	initial
inl	inlet wall
max	maximum
min	minimum
new	new
ng	natural gas
o	out
out	outlet
res	residual gas
$runner$	inlet runner
S	stroke
sg	stoichiometric gas
th	theoretical
tot	total
tr	trapped
$turb$	turbine
ub	unburned

1 Introduction

1.1. Background

The vast majority, roughly 90% of all internationally traded goods get to where they are going by sea. Transporting goods by ships is the most economic transportation mode, however shipping produces almost 1 billion metric ton CO2 per year. If shipping were a country it would be the sixth biggest greenhouse emitter [17]. In the reduction of the greenhouse problem the shipping world needs to play its part. According to the 3rd IMO GHG study, shipping emissions could under a business-as-usual scenario increase between 50% and 250% by 2050 [18]. Thus, the IMO strives to reduce total annual global shipping emissions by 50% over 2008 by 2050 [8]. Europe has set even more ambitious goals; in December 2019 The European commission published the Communication of the European green deal. This communication describes the goal of no net green house gasses in 2050 [5].

In addition to greenhouse gases, hazardous emissions such as sulfur oxides and nitrogen oxides need to be reduced. Sulphur has a major health and environmental impact, especially for populations living close to ports and coasts. Sulphur oxide can cause respiratory, cardiovascular and lung diseases in humans. Moreover, once sulphur oxide is released into the atmosphere it can cause acid rain which contributes to the acidification of the oceans and affects crops, forests and aquatic species [7]. Similar effect arise with nitrogen oxide emissions. It also contributes to acid depositions to the ocean and soil, which have a negative effect to the aquatic live and forests. In addition, the adverse effects of nitrogen oxide on the human health are, inflammation of the airways, reduced lung function and increasing susceptibility to respiratory infection [13]. Actions are made to reduce these hazardous gasses. On the first of January of 2020, a new sulphur limit on the sulphur content in the fuel oil used on board ships came into force. Known as “IMO 2020”, the rule limits the sulphur in the fuel oil used on board ships operating outside designated emission control areas to 0.50% m/m (mass by mass). This is a significant reduction from the previous limit of 3.5% [4]. The nitrogen limits are described in the NOX technical code 2008 by IMO. This code states the maximum allowed nitrogen emitted depending on the ship build year [12]. All these regulations are steps for a healthier environment, but require innovations in the shipping industry.

The use of alternative fuels such as ammonia, biofuels, hydrogen, liquefied natural gas (LNG), and methanol is one way to reduce greenhouse gases and hazardous emissions. Methanol is one of the most promising alternative fuels for several reasons [21]. First of all, methanol has a reasonable energy density, it requires more space and mass than diesel, but it has a higher energy density than other alternative fuels. Secondly, it burns cleaner. In laboratory testing Ellis and Tanneberger reported a potential 99% reduction in SOx and 60% reduction in NOx compared to traditional fuels [3]. Thirdly, currently most of the methanol is still produced by natural gas. But, methanol can also be produced by biomass or with renewable energy in carbon capture and utilisation schemes. So, due to the fact that burning methanol still emits CO2, but with the last production method CO2 is captured again, methanol has the potential to have zero net carbon emissions.

Other reasons why methanol is promising are that, from the fuels which are synthesized using renewable energy, it is the simplest fuel which is liquid at atmospheric conditions. Moreover, methanol is already produced world wide and lots of ports have already the infrastructure to accommodate methanol

fuel. Lastly, it does not rely on scarce resources. If produced by biomass, wood can be used. When produced by capturing CO2 only, water and energy (preferably renewable) is needed which we have plenty on earth. Thus, due to the fact that it is easy to handle since it‘s liquid at atmospheric conditions and there is already infrastructure in place and it does not rely on scarce recourse’s, makes that there are no bottlenecks to scale methanol to meet the global use [21].

Since, methanol is a promising fuel, it is already used in a couple of vessel. For example, the Stena Line ferry Stena Germanica uses a Wärstila engine since 2015 [22]. But, still a lot of research needs to be done before it overtakes the classic diesel fuels. For example as earlier stated, NOX and SOX can be reduced dramatically in laboratory facilities. But, how much is it reduced when applied in ships in different circumstances and loading conditions? Or, what about knocking? Similar to natural gas, methanol is sensitive to knocking [23]. Many more question about methanol combustion like these need to be answered before methanol can be globally used. Therefore, in The Netherlands the project MENENS was created by the Dutch government and companies in the shipping industry [10]. With this project the goal is to combine the expertise on methanol in the Netherlands to introduce methanol in the market as a fuel for zero-emission shipping.

On of the contributors to the MENENS project is the NLDA. In their lab they run a Caterpillar G3508 gas engine. It is a lean burn turbocharged marine SI natural gas engine with 8 cylinders and a rated power of 500kW. Other notable characteristics are, that is has zero valve overlap and the natural gas and air are mixed before the turbocharger. This engine is used to study different gaseous fuels. In the past, it was used on hydrogen and carbon dioxide blends with natural gas by Sapra [16] and eventually 100% methanol operation performed by Bosklopper [2]. Bosklopper investigated how the caterpillar engine could be converted to operate on 100% methanol. Moreover, he established the fuel consumption and NOx emissions at several loads. One of the conclusions made in this research was that, ”With increasing temperature after the cooler, lower NOx emissions can be realised”. He explains that, due to the higher temperature before the inlet valve more methanol evaporates. This causes better in-cylinder conditions. But, he only assumed this effect with one experimental test on 375kw and a 0-dimensional engine model. The engine model he used is based on the engine model created by Sapra [16], adapted to methanol. But, this model is focused on the in-cylinder process, not the induction process. Not only the temperature, but also the back pressure at the methanol inlet nozzle has an effect on the evaporation of the methanol and thus also the performance [2].

The theory behind NOx formation state that increasing the peak temperature increases the amount of NOx formation [19], [9]. Following that, by increasing the starting temperature and pressure the peak temperature increases as well [9]. The NOx formation should increase instead of decrease with increasing starting conditions. This is in contradiction on the statement of Bosklopper [2]. In this contradiction lies the knowledge gap for this thesis. Not many research has been done on the in-cylinder starting conditions of gas engines. Sapra developed a model that could predict the NOx formation of gas engine . But, he focused on the in-cylinder process. He didn‘t focus on the in-cylinder starting conditions, which have a large influence on the NOx production.

A parameter that describes all the in-cylinder starting conditions is the volumetric efficiency. The volumetric efficiency is a measure to evaluate the induction stroke of a four stroke engine as a gas pumping device [6]. Important parameters of the volumetric efficiency are the in-cylinder starting pressure and temperature. Thus, an engine model that can predict the volumetric efficiency with a decent accuracy can probably predict the NOx emissions accurately.

1.2. Research objective

The research objective of the thesis is to gain a better understanding of the starting conditions of the combustion process in order to accurately predict the performance parameters such as efficiency, CO_2 and NO_x emissions. The acquired knowledge on the starting conditions can then be used to further develop the 0-dimensional model of the Caterpillar G3508 gas engine, to better estimate the volumetric efficiency and later on the emissions. The existing model is developed by Sapra [15] and used by Bossklopper [2], but it focuses on the in-cylinder process. In this thesis, the induction estimation of the original model [15] will be improved to more accurately estimate the volumetric efficiency. Within this investigation, a focus needs to be given to the temperature flow during the induction stroke. The temperature has an effect on the evaporation of methanol and a large effect on the production of NOx gasses. Since, there are still a lot of questions on operating the Caterpillar G3508 gas engine on

methanol, the investigation will be done with natural gas fuel. Later on, this research can be the base to determine the volumetric efficiency of methanol based engines.

1.3. Research questions

The research objective can be translated into the following main research question: How can the estimation of the volumetric efficiency be improved of state of the art 0-dimensional spark ignited gas engine models?

To answer this question, the thesis is divided into several sub-questions:

- What is volumetric efficiency?
- What affects the volumetric efficiency?
- How can the volumetric efficiency be measured on the Caterpillar G3508 engine?
- Which effect do state of the art models take into account?
- How can the model be improved to more accurately estimate the volumetric efficiency on the caterpillar G3508 engine?
- What is the accuracy of the state of the art and the improved model?

1.4. Methodology

The methodology used to reach this goal is as follows. First, the theoretical background needed for this research is defined in chapter 3. Here, the definition of the volumetric efficiency is defined and a state of the art model is explained. Next, engine measurements are performed. The way the engine measurements are performed is explained in chapter 2. The engine measurements are used to investigate effects that are not yet included in the original model [15]. These effects are described in chapter 4. The effects are then incorporated into the original model to improve it‘s volumetric efficiency prediction. This is done in chapter 5. The experiments are also used to measure the volumetric efficiency. The volumetric efficiency can not directly be measured, but by measuring the exhaust emissions a good estimation of the volumetric efficiency can be made. This estimation is finally used to check the improved volumetric efficiency model in chapter 5.

2

The experimental set-up

2.1. Engine

The engine used for the experiments is a Caterpillar G3508 gas engine. It is a lean burn turbocharged marine SI natural gas engine with 8 cylinders and a rated power of 500 kW. In the past, it was used to study hydrogen and carbon dioxide blends with natural gas [16] and 100% methanol operation [2]. During the tests for this thesis, the engine was been operated on natural gas. This way, still unknown effects of different fuels don‘t need to be studied. Other notable characteristics are that is has zero valve overlap and the natural gas and air are mixed before the turbocharger. The table 2.1 displays the rest of the characteristics of the engine.

Table 2.1: Engine characteristics

Parameter	Value	Unit
Number of cylinders	8	-
Bore	0.17	m
Stroke	0.19	m
Rated power	500	kW
Rated speed	1500	rpm
compression ratio	12:1	-
Spark timing	24	°C ATDC
Inlet valve open	8.7	°C ATDC
Inlet valve close	21.5	°C ATDC
Exhaust valve open	20.1	°C BBDC
Exhaust valve close	11.8	°C BTDC

2.2. Flow

This chapter explains the flow of air and fuel in the test engine, which is important to determine the volumetric efficiency. Figure 2.1 provides a schematic overview of the engine. This chapter will shortly explain each component.

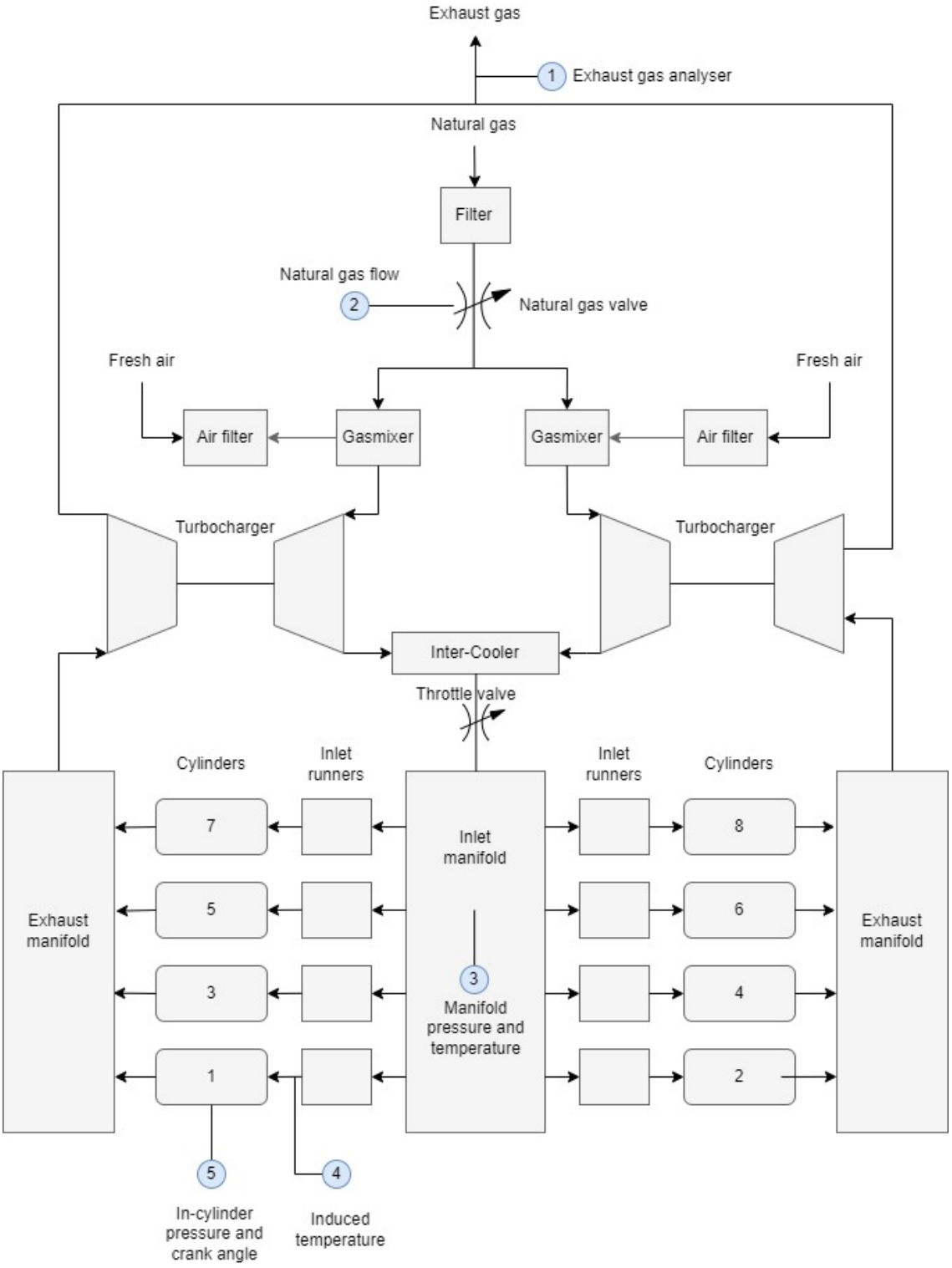

Figure 2.1: schematic overview of marine NG test engine setup [16]

- **Filter**
  The air and fuel are inducted in the engine through filters. The natural gas is supplied by the Dutch gas connection. The air inducted is inducted by two filters on the side of the engine. The filters clean the induced gas and create a little pressure drop.
- **Natural gas Valve**
  Between the natural gas filter and the gasmixer, there is a valve which controls the amounts of

natural gas that goes into the engine. Together with the throttle valve, it can control the air excess ratio in the engine.

- **Gas mixer**
  There are two gas mixers which mix the air with the natural gas and send it to the turbocharger.
- **Turbocharger**
  The goal of a turbocharger is to create more power per stroke for a given cylinder. To obtain more power, more fuel and combustion air need to be added during one cycle. To achieve this, the density of the mass needs to be increased by increasing the pressure. Thus, a turbocharger consists out of a compressor, which increases the pressure, and a turbine, which drives the compressor. This engine has two turbochargers. Each compressor of the turbochargers is driven by the hot exhaust gasses of 4 cylinders. The turbines, connected to the compressors, then increase the pressure of the gas mix received from the gas mixer and send it to the inter-cooler.
- **Inter-cooler**
  The function of the inter-cooler is to cool the hot compressed mixture, received from the turbocharger, before it enters the cylinder. The effect of the cooling of the mixture is that the density increases. This results in more mass of mixture inducted per induction stroke. The inter-cooler connects the two turbines with the throttle valve.
- **Throttle valve**
  The throttle valve controls the amount of gas inducted into the cylinders. Together with the natural gas valve, it also has another function. The combination of the two valves control the composition of the gas inducted into the cylinders. If the natural gas valve is relatively more open than the throttle valve, the mixture contains a lot of fuel. Thus, it is a rich mixture. If the natural gas valve is more closed relatively to the throttle valve, the mixture will contain more air. Thus, it is a lean mixture. This parameter is called the air fuel ratio (λ).
- **Inlet manifold**
  The inlet manifold is the volume where the mixture is gathered from the throttle valve. From this volume, it is directed to the cylinders via the inlet runner.
- **Inlet runner**
  The inlet runner is the connection from the inlet manifold to the cylinders. Since there are eight cylinders, there are also eight inlet runners.
- **Cylinders**
  This engine has eight cylinders in V-form, four on each side. In the cylinders, the combustion takes place. The mixture of natural gas and air received from the inlet manifold is combusted in the cylinder by a spark. The combusted mixture is then released to the two exhaust manifolds.
- **Exhaust manifold**
  The exhaust manifolds receive the exhaust gas from the cylinders and send it to the two compressors of the turbocharger. It is the area between the cylinder exhaust valves and the turbocharger.

2.3. Sensors

The engine is equipped with multiple sensors. The most important sensors for previous research projects on this engine were, the in-cylinder pressure and crank angle sensors. With these sensors the combustion process is determined. For this research not the combustion itself is important. In this research the end and starting conditions are investigated. To do this, senors are placed before and after the cylinder. The different data collected are temperature measurements, pressure measurements, flow measurements and emission measurements. A list of all sensors used with the location and accuracy can be found in table 2.2. The location of the sensors are also depicted in figure 2.1.

Table 2.2: Engine Sensors

Use	Sensor	Range	Accuracy	Location
Flow	Tecjet	-	6%	At Natural gas valve (2)
O_2%	Horiba PG-350E	0-25 vol%	0.175 vol%	After turbocharger (1)
CO_2%	Horiba PG-350E	0-20 vol%	0.1% vol%	After turbocharger (1)
NO_2%	Horiba PG-350E	0-250 ppm	2.5%	After turbocharger (1)
MAP	Dewetron pressure senor	0-10 bar	+/- 0.02 bar	In inlet manifold (3)
MAT	Thermo electra 1xK	0-1250 °C	+/- 2.2 °C	In inlet manifold (3)
T-induced	Thermo electra 1xK	0-1250 °C	+/- 2.2 °C	Before cylinder valve (4)
In-cylinder pressure	Kibox (kristler 7061B)	0-250 bar	+/- 1.25 bar	At cylinder head (5)
Crank angle	Kibox (Kistler 2614C/720)	-360°CA : +360°CA	+/- 0.23°CA	At the crank (5)

2.4. Test strategy

During the span of this research, the engine and senors were being rebuilt so no elaborate testing could take place. Tests were performed on two days. The first day, the engine was first run at 125kW for at least 10 min until the temperatures were stable. Then, the same was done for 250kW and 373kW. During the three load points, data from the installed sensors were gathered. The second test day the same procedure was followed but now for 116kW, 245kW, 364kW and 417kW.

3

Theoretical background

3.1. Volumetric efficiency

The volumetric efficiency is a dimensionless measure to evaluate the induction of a four stroke engine as a gas pumping device. Two stroke engines use different measures to evaluate the induction process since it includes scavenging. This chapter gives a definition of the volumetric efficiency and discusses effects which influence the volumetric efficiency.

3.1.1. Definition

Roussopoulos [14] has given a good general loose definition of the volumetric efficiency. He states that the volumetric efficiency is calculated by dividing the mass of the cylinder charge at some operating condition by the mass of charge that would occupy the cylinder at some standard gas conditions if the valve was left open and the piston stationary at bottom dead centre. More formal definitions differ per author.

Heywood [6] defines the volumetric efficiency by equation. Here $\dot{m_a}$ is the air mass flow in the cylinder, $\rho_{a,im}$ is the density of air at inlet manifold conditions, V_s is the stroke volume and N is the engine speed. In this definition the standard condition, to which the charge mass is compared, is the inlet manifold condition. Heywood ads that the charge mass can also be compared to atmospheric condition. Meaning, the density would be the atmospheric density.

$$\eta_v = \frac{\dot{m_a}}{\rho_{a,im} V_s N} \tag{3.1}$$

Taylor [20] uses a slightly different definition as can be seen in in equation 3.2. Where, $\dot{m_{im}}$ is the inlet mixture flow and ρ_{im} is the inlet density. Instead of only considering the air mass flow, he uses the fresh inlet flow mixture ($\dot{m_{im}}$). Similar to Heywood, Taylor states that the density can be taken at atmospheric conditions or at inlet manifold conditions.

$$\eta_v = \frac{\dot{m_{im}}}{\rho_{im} V_s N} \tag{3.2}$$

Roussopoulos [14] defines the volumetric efficiency as described in equation 3.3. Here, the residual gas flow $\dot{m_{res}}$ is included in the numerator. This has its use when only in-cylinder pressure data is available. With the in-cylinder pressure data only the total mass ($\dot{m_i} + \dot{m_{res}}$) can be calculated not the separate air mass or residual mass.

$$\eta_v = \frac{\dot{m_{im}} + \dot{m_{res}}}{\rho_{im} V_s N} \tag{3.3}$$

Lastly, Stapersma [19] does not define the volumetric efficiency as a fraction of masses but as a fraction of volumes. He states that the volumetric efficiency is the fraction between the induction volume

and the stroke volume as depicted in equation 3.4. Where, the induction volume v_{ind} is the volume inducted into the cylinder. It is only dependent on the inlet and outlet pressures and the valve timing. More about this effect in chapter 3.1.2.

$$\eta_v = \frac{V_{ind}}{V_s} \tag{3.4}$$

Stapersma [19] does introduce the extra parameter, filling efficiency. This parameter, he does define as the fraction between masses similar to the volumetric efficiency of the authors above. His definition is the mass drawn in the cylinder during induction relative to a theoretical mass based on inlet manifold conditions and stroke volume. Where, he defines the induction mass and the theoretical mass by the ideal gas law respectively for induction conditions and inlet manifold condition.

$$\eta_{fill} = \frac{m_{ind}}{m_{th}} \tag{3.5}$$

$$m_{ind} = \frac{p_{ind}V_{ind}}{R_{ind}T_{ind}} \tag{3.6}$$

$$m_{th} = \frac{p_{iman}V_s}{R_{iman}T_{iman}} \tag{3.7}$$

Most of the authors state that, the reference conditions can be taken at inlet manifold conditions or at atmospheric conditions. If the atmospheric conditions are chosen, the volumetric efficiency describes the induction process of the whole engine. If the inlet manifold is chosen as reference condition, the volumetric efficiency only describes the induction of the cylinder. For natural aspired engines, the ambient conditions are usually taken as reference conditions [6]. For turbocharged engines, the inlet manifold conditions are usually taken as reference conditions [1]. The reason is that, the turbocharger would otherwise have a very large effect on the volumetric efficiency. Instead, a turbocharged engines uses an efficiency for the turbocharger alone.

Each definition differs slightly in formulation and application, but they all describe the induction process of a four stroke engine. The absolute value of the volumetric efficiency is often not as important as the ability to compare the volumetric efficiency at different speeds loads or engines. Therefore, the most import thing is to be consistent in the definition when using the volumetric efficiency. Since, this thesis uses a turbocharged engine, where the natural gas and air are mixed before the turbocharger, the definition of Stapersma will be used with the inlet manifold conditions as the reference conditions. Where, the induction mass is the mixture of air and natural gas. This gives the following definition that will be used in this thesis (equation 3.8).

$$\eta_v = \frac{m_a + m_f}{\frac{p_{iman}V_s}{R_{iman}T_{iman}}} \tag{3.8}$$

3.1.2. Effects

In the following chapter, several effects are discussed, which affect the volumetric efficiency of a four stroke gas engine [6].

Air fuel ratio

For the volumetric efficiency definition used in this thesis, the air fuel ratio only affects the gas constant of the mixture. Since, a change in air fuel ratio causes a change in composition of the induced mass. If another definition would be used, it would also change the amount of induced mass. Since, the fuel takes in space that would otherwise be used by the air.

Heat transfer

The heat transfer can be described as the total heat pick-up from the gas. The heat pick-up can be split into two factors; the heat pick-up due to a warmer inlet runner and inlet valve and the mixing of fresh intake gas with hot residual gas.

The effect of heat pick-up of the gas to the cylinder is a decrease in volumetric efficiency. The explanation for this is the following. When the temperature in the cylinder is higher than the temperature

at standard condition, the density of the gas will decrease. If the density of the gas in the cylinder decreases, the mass in the cylinder will decrease. This leads to a decrease in volumetric efficiency.

Residual gas

As described in chapter 3.1.2, the hot residual gas effects the volumetric efficiency by heating up the incoming fresh air. But, this is not the only effect the residual gas has on the volumetric efficiency. Residual gas requires a certain volume in the cylinder that would otherwise be taken by the income fresh gas. Meaning a high amount of residual gas substantially decrease the volumetric efficiency.

Valve timing

Valve timing is the timing of the closing and opening of the inlet and exhaust valves. It has two effects.

Firstly, the valve timing affects the valve overlap. An engine has valve overlap when the inlet valve and exhaust valve are open at the same time. When, the pressure of the inlet manifold is higher than the pressure of the exit manifold, fresh gas will flow through the cylinder, otherwise called scavenging. When, the pressure of the exhaust valve is higher than the inlet manifold, combusted gas is pushed back into the inlet manifold, otherwise called back flow. The effect of back flow is that less fresh mixture is pushed into the cylinder. Thus, the volumetric efficiency decreases. The effect of scavenging is that residual gas is pushed out. Thus, creating more space for the fresh mixture. This leads to an increase in volumetric efficiency.

Secondly, if the inlet valve closes after bottom dead center, it could be that mass still enters the cylinder. This effect can occur when the inlet mass has a high momentum at high engine speeds. Due to the high momentum the mass is still pushed into the cylinder, even though the cylinder volume decreases. This effect is called ramming.

Friction losses

During the induction process the fresh mixture has to pass through valves and other obstruction. The friction of these obstruction leads to a decrease in pressure. When, the pressure in the cylinder is lower than the pressure at standard condition, the density of the mixture in the cylinder decreases. This leads to a decrease in volumetric efficiency.

Turbocharger

If the standard condition is taken at atmospheric conditions, the fresh mixture passes the turbocharger. The turbocharger then increases the pressure, which increases the density in the cylinder. Thus, more mass is induced into the cylinder. This leads to an increase in volumetric efficiency. Often, this effect increases the volumetric efficiency higher than one. Since, the goal of the volumetric efficiency is to describe the engine performance and not the turbocharger performance. For turbocharged engines the volumetric efficiency is calculated with the inlet manifold conditions as the standard condition. The inlet manifold is located after the turbocharger. Thus, the increase in pressure over the turbocharger has no effect on the volumetric efficiency.

3.2. State of the art model

There are multiple different models which model engines as explained in my literature study. Choosing the right model for the situation is very important. If a too simple model is chosen, certain variables or effects needed for the analysis won‘t be modelled. If a too complicated model is chosen, unnecessary effects and variables will be calculated. This will take up a lot of unnecessary time.

In this project an analyses of the effect of certain engine parameters on the volumetric efficiency will be investigated. This goal can be translated in three requirements of the model. The first requirement is that, engine parameters need to be modelled. This means a complete engine needs to be modelled. The second requirement is that, it can model the volumetric efficiency. This means that, the effects as discussed above need to be modelled in the engine. And Lastly, there are multiple engine parameters that will be investigated. Thus, the model needs to be fast.

Taking all of the requirements into account suitable models are 0-dimensional or 1-dimensional models. The test engine used for this thesis has already been used by Sapra [15]. He already made a 0-dimensional model. The model is focused on the in-cylinder process. But, it also describes the whole engine. It was not focused on the volumetric efficiency. So, not all effects are taken into account. But, it is a good basis. This chapter describes the model and lists areas where the model can be improved for

the calculation of the volumetric efficiency. From now on the model of Sapra will be called ”the original model”.

3.2.1. 0-dimensional original model

A schematic representation of the model can be seen in figure 3.2. The input of the model is the load, the composition of the fuel and the engine speed. First, based on the input parameters, the input fuel mass and Seiliger parameters are determined with parametric equations. Sapra derived these equation by performing elaborate engine tests at various loads. In the in-cylinder model the Seiliger parameters and fuel mass are used to calculate the power and heat generated by the engine. Besides the power and heat, the in-cylinder model also calculates the exhaust parameters. Exhaust parameters are the outlet pressure temperature and the gas composition at exit valve opening. The pressure and temperature are calculated by the Seiliger cycle and the mass composition is calculated by a mass and composition model. These models are elaborately explained in the paper of Sapra [16], but are not the focus of this thesis.

The pressure, temperature and gas composition at exit valve opening from the in-cylinder model are then the input for the turbocharger and exhaust receiver model. In this model the pressure and temperature after blowdown and after the compressor are calculated using the zinner blowdown, buchi balance and elliptic law.

Finally, the output data of the turbocharger and exhaust receiver model are used to determine the charge pressure and temperature which are inputs for the in-cylinder model. The working of this model is once again more elaborately explained in the chapter below.

This whole process is first estimated by a pre-simulation. The pre-simulation calculates, along with other variables, the initial brake power, which is compared to the input load. When the initial brake power is lower then the input power, the inlet manifold controller in the inlet manifold model will open the throttle by increasing the inlet manifold pressure. When the initial brake power is higher then the input power, the inlet manifold will decrease the pressure until the brake power is equal to the input power and stable.

For the calculation of the volumetric efficiency the input values of the in-cylinder model are important. These values are determined by initial estimations in the the manifold model. Below this model is explained. The in-cylinder model is less important. It will not be explained bellow, but can be found in the paper of Sapra [16].

Initial conditions

The initial conditions are gathered during a pre-simulation of the model. It starts with an estimation of the fuel mass, air excess ratio and the Seiliger parameters using parametric equations. Sapra identified trends in variations of combustion parameters to derive these parametric equations, specific to the used test engine, as a function of the load and other engine parameters. Figure 3.1 displays a schematic representation of these equations.

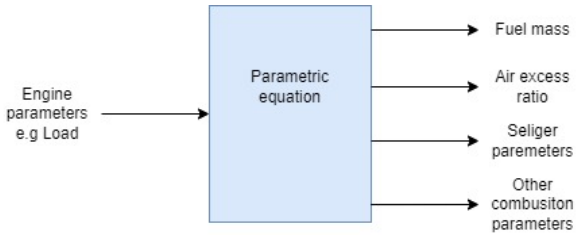

Figure 3.1: Parametric equations

Next, the initial inlet manifold pressure ($p_{Initial-im}$) is determined using equation 3.10. Where, ρ_{im} is the inlet mixture density, F_{fuel} is the volume fuel flow, σ_{vol} is the volume based stoichiometric air fuel ratio, λ is the air excess ratio, R_{im} is the inlet mixture gas constant, T_{im} is the inlet manifold temperature and V_{im} is the inlet manifold volume. This equation is based on the ideal gas law for the inlet manifold. The full derivation of this equation can be found in the work of Sapra [16]. The initial trapped pressure ($p_{initial-1}$) is assumed equal to the initial inlet manifold pressure.

$$p_{Initial-im} = \frac{\rho_{im} \cdot F_{fuel} \cdot (1 + \sigma_{vol} \cdot \lambda) \cdot R_{im} \cdot T_{im}}{V_{im}} \tag{3.9}$$

$$p_{Initial-im} = p_{initial-1} \tag{3.10}$$

The initial trapped temperature ($T_initial - 1$) is not calculated but estimated at 330K. With the trapped pressure and temperature, the initial trapped mass ($m_{initial-1}$) is calculated using the ideal gas law as in equation 3.11. Where, V_1 is the volume at inlet valve closing (trapped condition).

$$m_{initial-1} = \frac{p_{initial_1} \cdot V_1}{R_{im} \cdot T_{initial-1}} \tag{3.11}$$

With the initial trapped mass, fuel mass and air mass known the initial residual gas($m_{initial-res}$) is calculated with equation 3.12. With $m_{initial-f}$ and $m_{initial-a}$ respectively the input fuel mass and input air mass. The residual mass and fuel mass during the simulation will stay constant at every iteration. With a changing trapped mass, only the amount of air will change.

$$m_{initial-res} = m_{initial-1} - m_{initial-f} - m_{initial-a} \tag{3.12}$$

Inlet manifold model

In the inlet manifold model, the inlet manifold pressure is determined by a PI controller. The PI controller decrease or increases the pressure at every cycle until the calculated power is equal to the input power and stable. The PI controller increases the pressure if the calculated power is lower then the input power (simulating opening the throttle valve). When the calculated power is higher then the input power, the PI controller decreases the pressure (simulating closing of the throttle vale). The inlet manifold model also calculates the trapped temperature. This is an input for the in-cylinder model. The trapped temperature is calculated by taking the weighted average of the temperature of the induced mass and the residual mass temperature. The equation of the trapped temperature is given in equation 3.14. The full derivation of the equation can be found in the work of Stapersma [19]. In the equation; V_{IC}, V_{IO} and V_{EC} are respectively the volume at inlet valve closed, inlet valve open and exit valve closed. P_{iman} is the inlet manifold pressure as determined by the PI controller. $T_{turb,i}$ and $P_{turb,i}$ are respectively the turbine input temperature and pressure as determined by the Exhaust receiver and turbocharger model. T_{ind} is the induction temperature. The induction temperature is calculated by equation 3.13. Where $\epsilon_{inl} = 0.05$ is the heat exchange effectiveness and $T_{inl} = 400K$ is the inlet wall temperature.

$$T_{ind} = \epsilon_{inl} \cdot T_{inl} + (1 - \epsilon_{inl}) \cdot T_{man} \tag{3.13}$$

$$\frac{1}{T_1} = \frac{V_{IC} - V_{IO}}{V_{IC} \cdot T_{ind}} + \frac{V_{EC} \cdot P_d}{V_{IC} \cdot P_{iman} \cdot T_{turb,i}} \tag{3.14}$$

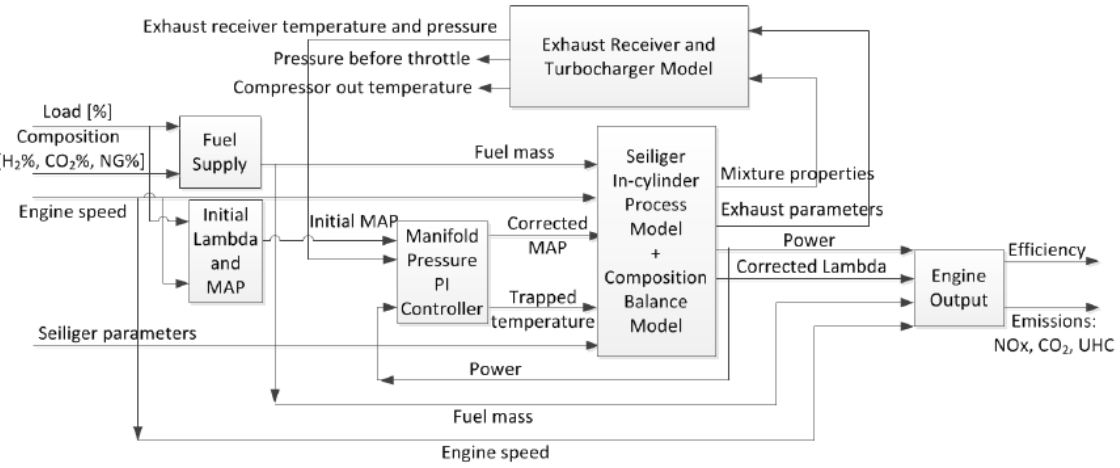

Figure 3.2: Schematic representation of the original mean value engine model [16]

4

Experimental results

In this chapter, the analyses of the experiments will be discussed. First, the inlet air is calculated using the emission measurements. With the inlet air also the fuel air ratio and the volumetric efficiency are calculated. Next, the change of the induction temperature depending on the load and pressure will be discussed. And finally, the pressure drop over the inlet valve is discussed.

Table 4.1: Test results day 1

Name	Unit	Test 1	Test 2	Test 3
Power	kW	125	250	373
NO_x	ppm	150	152	146
CO_2	vol%	6.35	6.42	6.34
O_2	vol%	9.41	9.22	9.56
Volume flow NG	Nm3/hr	63	103	146
T_{iman}	K	311.25	312.25	309.95
p_{iman}	kPa	73	118	163.8
T_{ind}	K	329-340	322-331	319-328
T_{ind}	K	334	326.5	323.5

Table 4.2: Test results day 2

Name	Unit	Test 1	Test 2	Test 3	Test 4	Test 5
Power	kW	116	245	364	417	0
NO_x	ppm	177	171	156	160	0
CO_2	vol%	7.66	7.39	7.25	7.33	0.06
O_2	vol%	7.22	7.73	8.08	8.05	20.94
Volume flow NG	Nm3/hr	61	98	136	159	0
T_{iman}	K	309.65	310.35	314.75	309.15	293.25
p_{iman}	kPa	72.5	117	164	181	100.8
T_{ind}	K	333.15-344.15	325.15-333.15	323.15-329.15	320.15-327.15	360.15-380.15
T_{ind}	K	338.65	329.15	326.15	323.65	370.15

4.1. Inducted mass

On the test engine, The tecjet measures the mass flow of natural gas. To know the mass inducted into the cylinders, also the air mass needs to be known. But, this is not directly measured on the engine. Rather then directly measuring the mass flow of air, the mass flow of air can also be calculated with the exhaust gas emissions as described by Stapersma in diesel engines volume 3 [19]. The exhaust emissions are measured on the test engine.

Stapersma [19] describes a way to calculate the air excess ratio from the inlet and outlet gas compositions. Stapersma did this for diesel fuel. In this chapter the method used in the book of Stapersma

is adapted to work for natural gas fuel. This air excess ratio can then be used to calculate the amount of inducted air.

The chapter is structured as follows. The chapter 4.1.1 describes the composition of dry air, wet air and natural gas. In chapter 4.1.2 the stoichiometric ratio of natural gas is determined. Next, in chapter 4.1.3 the composition of the inlet air and exhaust gas is determined. The last chapter 4.1.4 combines all the information from the previous chapters, to calculate the air excess ratio and the inducted mass.

4.1.1. Specification fuel and air

This chapter depicts the specifications of the fuel and air used in the test engine.

Dry air

Table 4.3 gives the composition of dry air [11]. Where, y depicts the mol fraction, x the mass fraction and M the molecular weight.

Table 4.3: Composition dry air [11]

Formula	y	x	M
N_2	0.78084	0.7551	28.0134
O_2	0.20946	0.2314	31.9988
Ar	0.00934	0.0129	39.9480
CO_2	0.000412	0.00062594	44.0098
Dry air	1	1	28.9677

The molecular weight of dry air is calculated with equation 4.1. Where, M_{da} , M_{N_2}, M_{O_2}, M_{Ar} and M_{CO_2} are respectively the molecular weight of dry air, nitrogen oxygen argon and carbon dioxide and $y^{da}_{N_2}$, $y^{da}_{O_2}$, y^{da}_{Ar} and $y^{da}_{CO_2}$ are respectively the mol fractions of nitrogen, oxygen, argon and carbon dioxide in dry air.

$$M_{da} = M_{N_2} \cdot y^{da}_{N_2} + M_{O_2} \cdot y^{da}_{O_2} + M_{Ar} \cdot y^{da}_{Ar} + M_{Ar} \cdot y^{da}_{CO_2} \tag{4.1}$$

Equations 4.2 to 4.5 depict the relation between x, y and M. Where, $x^{da}_{N_2}$,$x^{da}_{O_2}$,x^{da}_{Ar} and $x^{da}_{CO_2}$ are respectively the mass fraction of nitrogen, oxygen argon and carbon dioxide in dry air.

$$x^{da}_{N_2} = \frac{M_{N_2}}{M_{da}} \cdot y^{da}_{N_2} \tag{4.2}$$

$$x^{da}_{O_2} = \frac{M_{O_2}}{M_{da}} \cdot y^{da}_{O_2} \tag{4.3}$$

$$x^{da}_{Ar} = \frac{M_{Ar}}{M_{da}} \cdot y^{da}_{Ar} \tag{4.4}$$

$$x^{da}_{CO_2} = \frac{M_{CO_2}}{M_{da}} \cdot y^{da}_{CO_2} \tag{4.5}$$

Wet air

The amount of water in air is expressed as the absolute humidity in equation 4.6. Where, m_{H_2O} is the mass of water and m_{da} is the mass of dry air.

$$x^{da}_{H_2O} = \frac{m_{H_2O}}{m_{da}} \tag{4.6}$$

Equation 4.7 depicts the ratio between the mass of dry air and the mass of wet air. Where, m_a is the mass of the wet air and $m^{da}_{H_2O}$ is the mass of water in the air.

$$\frac{m_a}{m_{da}} = \frac{m_{da} + m^{da}_{H_2O}}{m_{da}} = 1 + x^{da}_{H_20} \tag{4.7}$$

With the relation in equation 4.7, equations 4.8 to 4.12 respectively calculate the mass fractions of nitrogen oxygen argon carbon dioxide and water of wet air.

$$x^a_{N2} = \frac{x^{da}_{N2}}{1 + x^{da}_{H_20}} \tag{4.8}$$

$$x^a_{O2} = \frac{x^{da}_{O2}}{1 + x^{da}_{H_20}} \tag{4.9}$$

$$x^a_{Ar} = \frac{x^{da}_{Ar}}{1 + x^{da}_{H_20}} \tag{4.10}$$

$$x^a_{CO_2} = \frac{x^{da}_{CO_2}}{1 + x^{da}_{H_20}} \tag{4.11}$$

$$x^a_{H_2O} = \frac{x^{da}_{H_2O}}{1 + x^{da}_{H_20}} \tag{4.12}$$

With the mass fraction, equation 4.13 calculates the molecular weight of wet air.

$$M_a = \frac{1}{\frac{x^a_{N2}}{M_{N_2}} + \frac{x^a_{O2}}{M_{O_2}} + \frac{x^a_{Ar}}{M_{Ar}} + \frac{x^a_{CO2}}{M_{CO_2}} + \frac{x^a_{H_2O}}{M_{H_2O}}} \tag{4.13}$$

Finally, equations 4.14 to 4.18 respectively calculated the mol fractions of the nitrogen oxygen argon, carbon dioxide and water in wet air.

$$y^a_{N_2} = \frac{M_a}{M_{N_2}} \cdot x^a_{N_2} \tag{4.14}$$

$$y^a_{O_2} = \frac{M_a}{M_{O_2}} \cdot x^a_{O_2} \tag{4.15}$$

$$y^a_{Ar} = \frac{M_a}{M_{Ar}} \cdot x^a_{Ar} \tag{4.16}$$

$$y^a_{CO_2} = \frac{M_a}{M_{CO_2}} \cdot x^a_{CO_2} \tag{4.17}$$

$$y^a_{H_2O} = \frac{M_a}{M_{H_2O}} \cdot x^a_{H_2O} \tag{4.18}$$

Table 4.4 [11] gives an overview of the mass fraction, mol fraction and molecular weight of wet air.

Table 4.4: Composition wet air [11]

Formula	y	x	M
N_2	0.7719	0.7498	28.0134
O_2	0.2071	0.2298	31.9988
Ar	0.0092	0.0127	39.9480
CO_2	0.0003	0.00045783	44.0098
H_2O	0.0115	0.0072	18.0152
Wet air	1	1	28.8384

Table 4.5: Composition natural gas [11]

Formula	y	x	M
CH_4	0.8075	0.6812	22.36
C_2H_6	0.0317	0.0501	33.1874
C_3H_8	0.00792	0.0184	21.9297
$i-C_4H_{10}$	0.001672	0.00511	21.6104
$n-C_4H_{10}$	0.0019	0.005807	21.6104
$i-C_5H_{12}$	0.00073	0.00277	21.0838
$n-C_5H_{12}$	0.000447	0.001696	21.0838
$i-C_6H_{14}$	0.0001465	0.000664	20.5
$n-C_6H_{14}$	0.0001121	0.000508	20.5
C_6H_6	0.000151	0.000620	20.5
He	0.000267	0.00005619	22.4248
Ar	0.0001	0.00021007	22.3925
H	0.000013	0.00000069	1.0079
N_2	0.1267	0.1866	28.0134
CO_2	0.02005	0.0464	44.0098
Natural gas	1	1	19.0162

Natural gas

During the tests, the engine uses Groningen natural gas as fuel. Table 4.5 [11] depicts the composition of the gas in mol fraction (y), mass fraction (x) and molecular weight (M).

The composition of natural gas can also be described as fractions of the elements carbon, hydrogen, nitrogen and oxygen. This makes it easier to calculate with and, will be used in the next chapters. The mass fraction of nitrogen stays the same because it only occurs in one form. Equations 4.19, 4.20 and 4.21 respectively calculate The mass fraction of hydrogen carbon and oxygen.

$$\begin{aligned} x_H^{NG} = {} & x_{CH_4}^{NG}\frac{4 * M_H}{M_{CH_4}} + x_{C_2H_6}^{NG}\frac{6 \cdot M_H}{M_{C_2H_6}} + x_{C_3H_8}^{NG}\frac{8 \cdot M_H}{M_{C_3H_8}} + (x_{i-C_4H_10}^{NG} + x_{n-C_4H_10}^{NG})\frac{10 \cdot M_H}{M_{i-C_4H_10}} \\ & + (x_{i-C_5H_12}^{NG} + x_{n-C_5H_12}^{NG})\frac{12 \cdot M_H}{M_{i-C_5H_12}} + (x_{i-C_6H_14}^{NG} + x_{n-C_6H_14}^{NG})\frac{14 \cdot M_H}{M_{i-C_6H_14}} + x_{C_6H_6}^{NG}\frac{6 \cdot M_H}{M_{C_6H_6}} \end{aligned} \tag{4.19}$$

$$\begin{aligned} x_C^{NG} = {} & x_{CH_4}^{NG}\frac{1 \cdot M_C}{M_{CH_4}} + x_{C_2H_6}^{NG}\frac{2 \cdot M_C}{M_{C_2H_6}} + x_{C_3H_8}^{NG}\frac{3 \cdot M_C}{M_{C_3H_8}} + (x_{i-C_4H_10}^{NG} + x_{n-C_4H_10}^{NG})\frac{4 \cdot M_C}{M_{C_4H_10}} \\ & + (x_{i-C_5H_12}^{NG} + x_{n-C_5H_12}^{NG})\frac{5 \cdot M_C}{M_{C_5H_12}} + (x_{i-C_6H_14}^{NG} + x_{n-C_6H_14}^{NG} + x_{C_6H_6}^{NG})\frac{6 \cdot M_C}{M_{C_6H_14}} + x_{CO_2}^{NG}\frac{1 \cdot M_C}{M_{CO_2}} \end{aligned} \tag{4.20}$$

$$x_{O_2}^{NG} = x_{O_2}^{NG} + x_{CO_2}^{NG}\frac{M_{O_2}}{M_{CO_2}} \tag{4.21}$$

4.1.2. Stoichiometric air fuel ratio

Natural gas consists mainly out of carbon, hydrogen and nitrogen atoms. It is assumed that all the carbon and hydrogen combusts and part of the nitrogen. The reaction equations of C, H and N for the respective amounts of mol are given in equations 4.22, 4.23 and 4.24. Where, n_C^f and n_H^f are respectively the amount of mol carbon and hydrogen in the fuel and $n_{b-N_2}^{im}$ is the amount of nitrogen burned.

$$n_C^f \cdot C + n_C^f \cdot O_2 \rightarrow n_C^f \cdot CO_2 \tag{4.22}$$

$$n_h^f \cdot H + \frac{1}{4}n_H^f \cdot O_2 \rightarrow \frac{1}{2}n_H^f \cdot H_2O \tag{4.23}$$

$$n^{im}_{b-N_2} \cdot N_2 + 2n^{im}_{b-N_2} \cdot O_2 \rightarrow 2n^{im}_{b-N_2} \cdot NO_2 \tag{4.24}$$

Using the reaction equation, the amount of oxygen required is given in equation 4.25. Where, m_f is the amount of fuel and $x^{im}_{b-N_2}$ is the mass fraction of the amount of nitrogen burned in the inlet.

$$\begin{aligned} n^{min}_{O2} &= n^f_C + \frac{1}{4}n^f_H + 2n^{im}_{b-N_2} \\ &= (\frac{x^f_C}{M_C} + \frac{1}{4}\frac{x^f_H}{M_h}) \cdot m_f + 2\frac{x^{im}_{b-N_2}}{M_{N_2}} \cdot m_{im} \end{aligned} \tag{4.25}$$

To simplify equation 4.25 the inlet mass should be replaced by the fuel mass. Therefore, equation 4.28 is created by combining equation 4.26 and 4.27. Where, $x^f_{b-N_2}$ is the total amount of burned nitrogen in the inlet compared to the fuel mass.

$$x^f_{b-N_2} = \frac{m^{im}_{b-N_2}}{m_f} \tag{4.26}$$

$$x^{im}_{b-N_2} = \frac{m^{im}_{b-N_2}}{m_{im}} \tag{4.27}$$

$$x^{im}_{b-N_2} = x^f_{b-N_2} \cdot \frac{m_f}{m_{im}} \tag{4.28}$$

With equation 4.28 equation 4.25 is rewritten, such that it no longer contains the inlet mass.

$$n^{mim}_{O2} = (\frac{x^f_C}{M_C} + \frac{1}{4}\frac{x^f_H}{M_h} + 2\frac{x^f_{b-N_2}}{M_{N_2}}) \cdot m_f \tag{4.29}$$

In the fuel there is only 0.02 % oxygen. This percentage is so small the air in the fuel is neglected. Meaning that all the oxygen must be supplied by the air:

$$n^{min}_{O2} = n^{a-min}_{O2} \tag{4.30}$$

The minimum required amount of oxygen is expressed in the minimum required amount of air or dry air in equation 4.31. Where, m_{a-min} is the minimum amount of wet air in kg and m_{da-min} is the minimum amount of dry air in kg.

$$\begin{aligned} n^{a-min}_{O2} &= y^a_{O_2} \cdot \frac{m_{a-min}}{M_a} \\ &= y^{da}_{O_2} \cdot \frac{m_{da-min}}{M_{da}} \end{aligned} \tag{4.31}$$

By definition the stoichiometric air fuel ratio is:

$$\sigma = \frac{m_{a-min}}{m_f} \tag{4.32}$$

Or for dry air:

$$\sigma_d = \frac{m_{da-min}}{m_f} \tag{4.33}$$

Thus, by dividing equations 4.31 and 4.29, the stoichometric air fuel ratio for dry and wet air is calculated:

$$\sigma = \frac{M_a}{y^a_{O_2}} \cdot (\frac{X^f_C}{M_C} + \frac{1}{4}\frac{X^f_H}{M_h} + 2\frac{X^f_{b-N_2}}{M_{N_2}}) \tag{4.34}$$

$$\sigma_{da} = \frac{M_{da}}{y^{da}_{O_2}} \cdot (\frac{x^f_C}{M_C} + \frac{1}{4}\frac{x^f_H}{M_h} + 2\frac{x^f_{b-N_2}}{M_{N_2}}) \tag{4.35}$$

4.1.3. Composition exhaust

In this chapter the amount of mol needed per kg fuel is determined for each reactant in the inlet air and exhaust gas.

Nitrogendioxide

In air and natural gas a considerable amount of nitrogen can be found. The sum of these two gives the total amount of nitrogen in the inlet (equation 4.36). During combustion, some nitrogen will burn and form NO, NO_2 and NO_3. In reality most nitrogen will burn to NO_2 [19]. For simplification, only the formation of NO_2 is modelled. Equation 4.37 gives the relation of burned and unburned nitrogen. Where, n^{im}_{N2} is the total amount of nitrogen in the air and natural gas combined, n^{im}_{ub-N2} is the amount of nitrogen which is not burned during combustion and n^{im}_{b-N2} is the amount of nitrogen burned during combustion.

$$n^{im}_{N2} = n^{a}_{N2} + n^{f}_{N2} \tag{4.36}$$

$$n^{im}_{N2} = n^{im}_{ub-N2} + n^{im}_{b-N2} \tag{4.37}$$

In equation 4.38, the amount of nitrogen dioxide in the exhaust caused by the burned nitrogen is determined from the nitrogen balance.

$$n^{im}_{b-N2} \cdot N_2 + 2n^{im}_{b-N2} \cdot O_2 \rightarrow 2n^{im}_{b-N2} \cdot NO_2 \tag{4.38}$$

From this balance can be concluded that, the amount of mol of nitrogen dioxide in the exhaust is double to the amount of nitrogen burned.

$$\begin{aligned} \dot{n}^{g-out}_{NO_2} &= 2\dot{n}^{im}_{b-N2} \\ &= 2\frac{\dot{m}^{im}_{b-N2}}{M_{N_2}} \\ &= 2\frac{x^{f}_{b-N2}}{M_{N_2}} \cdot \dot{m}_f \end{aligned} \tag{4.39}$$

In equation 4.40, this is rewritten as mol per kg fuel. Where, $\dot{nr}^{g-out}_{NO_2}$ is the amount of nitrogen dioxide mol in the exhaust per kg fuel.

$$\dot{nr}^{g-out}_{NO_2} = 2\frac{x^{f}_{b-N2}}{M_{N_2}} \tag{4.40}$$

Nitrogen

Some nitrogen will burn to nitrogen dioxide, as explained in the chapter above, and some nitrogen will not react. This means the nitrogen in the exhaust gas is the nitrogen in the air plus the nitrogen in the fuel minus the unburned nitrogen. In equation 4.41, this is rewritten in multiple forms .Where, $\dot{m^{f}_{N_2}}$ is the mass flow of nitrogen in the fuel.

$$\begin{aligned} \dot{n}^{g-out}_{N_2} &= \dot{n}^{a-im}_{N_2} + \dot{n}^{f}_{N_2} - \dot{n}^{im}_{b-N2} \\ &= y^{a-im}_{N_2} \cdot \dot{n}_{a-im} + \frac{\dot{m^{f}_{N_2}}}{M_{N_2}} - \frac{\dot{m}^{im}_{b-N2}}{M_{N_2}} \\ &= \frac{y^{a-im}_{N_2}}{M_a} \cdot \dot{m}_{a-im} + \frac{x^{f}_{N_2}}{M_{N_2}} \cdot \dot{m}_f - \frac{\dot{x^{f}_{b-N2}}}{M_{N_2}} \cdot \dot{m}_f \\ &= \frac{y^{a-im}_{N_2}}{M_a} \cdot \lambda_{tot} \cdot \sigma \cdot \dot{m}_f + (\frac{x^{f}_{N_2}}{M_{N_2}} - \frac{\dot{x^{f}_{b-N2}}}{M_{N_2}}) \cdot \dot{m}_f \end{aligned} \tag{4.41}$$

This gives the mol flow of nitrogen per kg fuel flow:

$$\begin{aligned} \dot{nr}_{N_2}^{g-out} &= \frac{y_{N_2}^{a-im}}{M_a} \cdot \lambda_{tot} \cdot \sigma + \frac{x_{N_2}^f}{M_{N_2}} - \frac{\dot{x_{b-N2}^f}}{M_{N_2}} \\ &= \frac{y_{N_2}^{da-im}}{M_{da}} \cdot \lambda_{tot} \cdot \sigma_{da} + \frac{x_{N_2}^f}{M_{N_2}} - \frac{\dot{x_{b-N2}^f}}{M_{N_2}} \end{aligned} \tag{4.42}$$

Oxygen

If complete combustion is assumed, equation 4.43 depicts the mol flow of oxygen for exhaust air. Where, $n_{O_2}^{a-comb}$ is the air used during combustion.

$$\begin{aligned} \dot{n}_{O_2}^{g-out} &= \dot{n}_{O_2}^{a-im} - \dot{n}_{O_2}^{a-comb} \\ &= y_{O_2}^{a-im} \cdot (\dot{n}_{a-im} - \dot{n}_{a-comb}) \\ &= \frac{y_{O_2}^{a-im}}{M_a} \cdot (\dot{m}_{a-im} - \dot{m}_{a-comb}) \\ &= \frac{y_{O_2}^{a-im}}{M_a} \cdot (\lambda_{tot} - 1) \cdot \sigma \cdot \dot{m}_f \end{aligned} \tag{4.43}$$

This gives the mol flow of oxygen for per kg fuel flow:

$$\begin{aligned} \dot{nr}_{O_2}^{g-out} &= \frac{y_{O_2}^{a-im}}{M_a} \cdot (\lambda_{tot} - 1) \cdot \sigma \\ &= \frac{y_{O_2}^{da-im}}{M_{da}} \cdot (\lambda_{tot} - 1) \cdot \sigma_{da} \end{aligned} \tag{4.44}$$

Ar

Argon is not involved in any reaction since it‘s a noble gas. Thus, the amount of argon in the exhaust is equal to the amount of argon in the inlet:

$$\begin{aligned} \dot{nr}_{Ar}^{g-out} &= \dot{nr}_{Ar}^{a-im} \\ &= y_{Ar}^{a-im} \cdot \dot{n}_{a-im} \\ &= \frac{y_{Ar}^{a-im}}{M_a} \cdot \dot{m}_{a-im} \\ &= \frac{y_{Ar}^{a-im}}{M_a} \cdot \lambda_{tot} \cdot \sigma \cdot \dot{m}_f \end{aligned} \tag{4.45}$$

This gives the mol flow of argon per kg fuel flow:

$$\begin{aligned} \dot{nr}_{Ar}^{g-out} &= \frac{y_{Ar}^{a-im}}{M_a} \cdot \lambda_{tot} \cdot \sigma \\ &= \frac{y_{Ar}^{da-im}}{M_{da}} \cdot \lambda_{tot} \cdot \sigma_{da} \end{aligned} \tag{4.46}$$

Carbon dioxide

The amount of carbon dioxide in the exhaust is determined from the carbon balance:

$$n_C^f \cdot C + n_C^f \cdot O_2 \rightarrow n_C^f \cdot CO_2 \tag{4.47}$$

From this balance can be concluded that, the amount of mol of carbon dioxide in the exhaust is equal to the amount of carbon in the fuel:

$$\begin{aligned}\dot{n}_{CO_2}^{g-out} &= \dot{n_C^f} \\ &= \frac{\dot{m_C^f}}{M_C} \\ &= \frac{x_C^f}{M_C} \cdot \dot{m}_f\end{aligned} \tag{4.48}$$

Thus, for the amount of carbon dioxide in the exhaust per kg fuel:

$$\dot{nr}_{CO_2}^{g-out} = \frac{x_C^f}{M_C} \tag{4.49}$$

Water

The amount of water in the exhaust as produced by combustion can be calculated with the hydrogen balance:

$$n_H^f \cdot H + \frac{1}{4} n_H^f \cdot O_2 \rightarrow \frac{1}{2} n_H^f \cdot H_2O \tag{4.50}$$

From this balance can be concluded that, the amount of mol of water in the exhaust, as produced by combustion, is half of the amount of hydrogen in the fuel. To get the total amount of water the amount already present in the air must be added.

$$\begin{aligned}\dot{n}_{H_2O}^{g-out} &= \frac{1}{2} \cdot \dot{n_H^f} + \dot{n}_{H_2O}^{a-im} \\ &= \frac{1}{2} \cdot \frac{\dot{m_H^f}}{M_H} + \frac{y_{H_2O}^{a-im}}{M_a} \cdot \dot{m}_{a-im} \\ &= \frac{1}{2} \cdot \frac{x_H^f}{M_H} \cdot \dot{m}_f + \frac{y_{H_2O}^{a-im}}{M_a} \cdot \lambda_{tot} \cdot \sigma \cdot \dot{m}_f\end{aligned} \tag{4.51}$$

This gives for the amount of water in the exhaust per kg fuel:

$$\begin{aligned}\dot{nr}_{H_2O}^{g-out} &= \frac{1}{2} \cdot \frac{x_H^f}{M_H} + \frac{y_{H_2O}^{a-im}}{M_a} \cdot \lambda_{tot} \cdot \sigma \\ &= \frac{1}{2} \cdot \frac{x_H^f}{M_H} + \frac{y_{H_2O}^{da-im}}{M_{da}} \cdot \lambda_{tot} \cdot \sigma_{da} \\ &= \frac{1}{2} \cdot \frac{x_H^f}{M_H} + \frac{x_{H_2O}^{da-im}}{M_{H_2O}} \cdot \lambda_{tot} \cdot \sigma_{da}\end{aligned} \tag{4.52}$$

Sum of all reactants

Table 4.6 gives an overview of the mol balance in the inlet air and exhaust relative to the fuel.

Table 4.6: Overview mol balance in mol ratio relative to the fuel

element	air in		exhaust
N_2	$\frac{y_{N_2}^{da-im}}{M_{da}} \cdot \lambda_{tot} \cdot \sigma_{da}$	$\rightarrow$	$\frac{y_{N_2}^{da-im}}{M_{da}} \cdot \lambda_{tot} \cdot \sigma_{da} + \frac{x_{N_2}^f}{M_{N_2}} - \frac{x_{b-N_2}^f}{M_{N_2}}$
O_2	$\frac{y_{O_2}^{da-im}}{M_{da}} \cdot \lambda_{tot} \cdot \sigma_{da}$	$\rightarrow$	$\frac{y_{O_2}^{a-im}}{M_d a} \cdot (\lambda_{tot} - 1) \cdot \sigma_{da}$
Ar	$\frac{y_{Ar}^{da-im}}{M_{da}} \cdot \lambda_{tot} \cdot \sigma_{da}$	$\rightarrow$	$\frac{y_{Ar}^{da-im}}{M_{da}} \cdot \lambda_{tot} \cdot \sigma_{da}$
CO_2	-	$\rightarrow$	$\frac{x_C^f}{M_C}$
NO_2	-	$\rightarrow$	$2\frac{x_{b-N_2}^f}{M_{N_2}}$
H_2O	$\frac{x_{H_2O}^{da-im}}{M_{H_2O}} \cdot \lambda_{tot} \cdot \sigma_{da}$	$\rightarrow$	$\frac{1}{2} \cdot \frac{x_H^f}{M_H} + \frac{x_{H_2O}^{da-im}}{M_{H_2O}} \cdot \lambda_{tot} \cdot \sigma_{da}$
sum	$\frac{\lambda_{tot} \cdot \sigma_{da}}{M_{da}} + \frac{x_{H_2O}^{da-im}}{M_{H_2O}} \cdot \lambda_{tot} \cdot \sigma_{da}$	$\rightarrow$	$nr_{wet}^{a-im} + \frac{1}{4} \cdot \frac{x_H^f}{M_H} + \frac{x_{N_2}^f}{M_{N_2}} - \frac{x_{b-N_2}^f}{M_{N_2}}$

The total mol in the inlet air is:

$$\begin{aligned} nr_{wet}^{a-im} &= \frac{y_{N_2}^{da-im}}{M_{da}} \cdot \lambda_{tot} \cdot \sigma_{da} + \frac{y_{O_2}^{da-im}}{M_{da}} \cdot \lambda_{tot} \cdot \sigma_{da} + \frac{y_{Ar}^{da-im}}{M_{da}} \cdot \lambda_{tot} \cdot \sigma_{da} + \frac{x_{H_2O}^{da-im}}{M_{H_2O}} \cdot \lambda_{tot} \cdot \sigma_{da} \\ &= \frac{\lambda_{tot} \cdot \sigma_{da}}{M_{da}} + \frac{x_{H_2O}^{da-im}}{M_{H_2O}} \cdot \lambda_{tot} \cdot \sigma_{da} \end{aligned} \tag{4.53}$$

The sum of the mol in the exhaust gas is:

$$\begin{aligned} nr_{wet}^{g-out} &= \frac{\lambda_{tot} \cdot \sigma_{da}}{M_{da}} - \frac{y_{O_2}^{da-im} \cdot \sigma_{da}}{M_{da}} + \frac{x_C^f}{M_C} + \frac{1}{2} \cdot \frac{x_H^f}{M_H} + \frac{x_{H_2O}^{da-im}}{M_{H_2O}} \cdot \lambda_{tot} \cdot \sigma_{da} + \frac{x_{N_2}^f}{M_{N_2}} + \frac{x_{b-N_2}^f}{M_{N_2}} \\ &= nr_{wet}^{a-im} - \frac{y_{O_2}^{da-im} \cdot \sigma_{da}}{M_{da}} + \frac{x_C^f}{M_C} + \frac{1}{2} \cdot \frac{X_H^f}{M_H} + \frac{x_{N_2}^f}{M_{N_2}} + \frac{x_{b-N_2}^f}{M_{N_2}} \end{aligned} \tag{4.54}$$

Replacing sigma by equation 4.35 in equation 4.54 gives:

$$\begin{aligned} nr_{wet}^{g-out} &= nr_{wet}^{air-im} + \frac{x_C^f}{M_C} + \frac{1}{2} \cdot \frac{x_H^f}{M_H} + \frac{x_{N_2}^f}{M_{N_2}} + \frac{x_{b-N_2}^f}{M_{N_2}} - (\frac{x_C^f}{M_C} + \frac{1}{4}\frac{x_H^f}{M_h} + 2\frac{x_{b-N_2}^f}{M_{N_2}}) \\ &= nr_{wet}^{a-im} + \frac{1}{4} \cdot \frac{x_H^f}{M_H} + \frac{x_{N_2}^f}{M_{N_2}} - \frac{x_{b-N_2}^f}{M_{N_2}} \\ &= \frac{\lambda_{tot} \cdot \sigma_{da}}{M_{da}} + \frac{x_{H_2O}^{da-im}}{M_{H_2O}} \cdot \lambda_{tot} \cdot \sigma_{da} + \frac{1}{4} \cdot \frac{x_H^f}{M_H} + \frac{x_{N_2}^f}{M_{N_2}} - \frac{x_{b-N_2}^f}{M_{N_2}} \end{aligned} \tag{4.55}$$

For dry air the water in the exhaust is removed:

$$\begin{aligned} nr_{dry}^{g-out} &= \frac{\lambda_{tot} \cdot \sigma_{da}}{M_{da}} + \frac{x_{H_2O}^{da-im}}{M_{H_2O}} \cdot \lambda_{tot} \cdot \sigma_{da} + \frac{1}{4} \cdot \frac{x_H^f}{M_H} + \frac{x_{N_2}^f}{M_{N_2}} - \frac{x_{b-N_2}^f}{M_{N_2}} - \frac{x_{H_2O}^{da-im}}{M_{H_2O}} \cdot \lambda_{tot} \cdot \sigma_{da} - \frac{1}{2}\frac{x_H^f}{M_h} \\ &= \frac{\lambda_{tot} \cdot \sigma_{da}}{M_{da}} - \frac{1}{4}\frac{x_H^f}{M_h} + \frac{x_{N_2}^f}{M_{N_2}} - \frac{x_{b-N_2}^f}{M_{N_2}} \end{aligned} \tag{4.56}$$

4.1.4. Induction mass

Dividing equation 4.44 by equation 4.56 gives the mol fraction O_2 in the exhaust:

$$y_{O_2}^{dg-out} = \frac{\frac{y_{O_2}^{a-im}}{M_{da}} \cdot (\lambda_{tot} - 1) \cdot \sigma_{da}}{\frac{\lambda_{tot} \cdot \sigma_{da}}{M_{da}} - \frac{1}{4}\frac{x_H^f}{M_h} + \frac{x_{N_2}^f}{M_{N_2}} - \frac{x_{N_2}^b}{M_{N_2}}} \tag{4.57}$$

Rewriting this to λ gives:

$$\lambda_{tot} = \frac{y_{O_2}^{da-im} - y_{O_2}^{dg-out}\frac{M_{da}}{\sigma_{da}}(\frac{1}{4}\frac{x_H^f}{M_H} - \frac{x_{N_2}^f}{M_{N_2}} + \frac{x_{N_2}^b}{M_{N_2}})}{y_{O_2}^{da-im} - y_{O_2}^{dgout}} \tag{4.58}$$

Since the amount of fuel is measured, the amount of air can be calculated with the new air excess ratio.

$$m_a = \lambda \cdot m_f \tag{4.59}$$

With the amount of air known, the total inducted mass is the sum of the amount of air and the amount of fuel:

$$m_{im} = m_a + m_f \tag{4.60}$$

Now following the definition of volumetric efficiency that is used in this paper:

$$\eta_{vol} = \frac{m_a + m_f}{\frac{p_{iman} V_{iman}}{R_m ix \cdot T_{iman}}} \tag{4.61}$$

Results

Using equations 4.58, 4.59, 4.60 4.61 and the test data, tables 4.8 and 4.7 calculate and display all the mass flows and volumetric efficiency for the test results.

Table 4.7: Mass flows test day 2

Name	Unit	Test 116kW	Test 245kW	Test 364kW	Test 417kW
Inducted air mass flow	kg/s	0.275	0.458	0.651	0.760
Inducted fuel mass flow	kg/s	0.014	0.023	0.031	0.037
Inducted mass flow	kg/s	0.289	0.480	0.683	0.797
Volumetric efficiency	-	87%	90%	92%	96%

Table 4.8: Mass flows test day 1

Name	Unit	Test 125kW	Test 250kW	Test 373kW
Inducted air mass flow	kg/s	0.335	0.539	0.785
Inducted fuel mass flow	kg/s	0.015	0.024	0.034
Inducted mass flow	kg/s	0.349	0.562	0.819
Volumetric efficiency	-	104%	104%	108%

As can be seen in table 4.8, the volumetric efficiency is higher then 100%. This is not a logical results. As explained in chapter 3.1.2, only the turbocharger can cause a volumetric efficiency higher then 100%. But, the definition used for the volumetric efficiency has the manifold inlet conditions as the reference condition. Thus, the turbocharger has no effect on the volumetric efficiency. The explanation of the results can be found in the test conditions. During the first test, old exhaust calibrating tanks were used. Before the second test, new tanks were installed. This means the absolute values of the exhaust emissions measured during the first test are wrong. To still calculate the inducted mass of the first experiment the air fuel ratio of the second experiment is used to calculated the inducted air mass for the second experiment. table 4.9 displays the new results. The volumetric efficiency is still

higher then the volumetric efficiency of experiment two but, it is lower then one. In the remainder of this research the corrected mass of experiment will be used.

Table 4.9: Mass flows test day 1 corrected

Name	Unit	Test 125kW	Test 250kW	Test 373kW
Inducted air mass flow	kg/s	0.284	0.481	0.699
Inducted fuel mass flow	kg/s	0.015	0.024	0.034
Inducted mass flow	kg/s	0.298	0.505	0.733
Volumetric efficiency	-	89%	94%	97%

4.2. Induction temperature

The induction temperature is the temperature of the mixture which is inducted into the cylinder. This temperature is not yet the trapped temperature of the whole mixture at inlet valve closing. The trapped temperature will be a bit higher since the trapped mass is the inducted mixture mixed with the residual gas still in the cylinder. During the measurements, the induction temperature is measured just before the inlet valve. The actual induction temperature will be a bit higher, since the mixture still has to pass the very hot inlet valve. But, this is the closest place where the induction temperature could be measured. If, the temperature measurement would be taken after the cylinder valve, the trapped temperature would be measured.

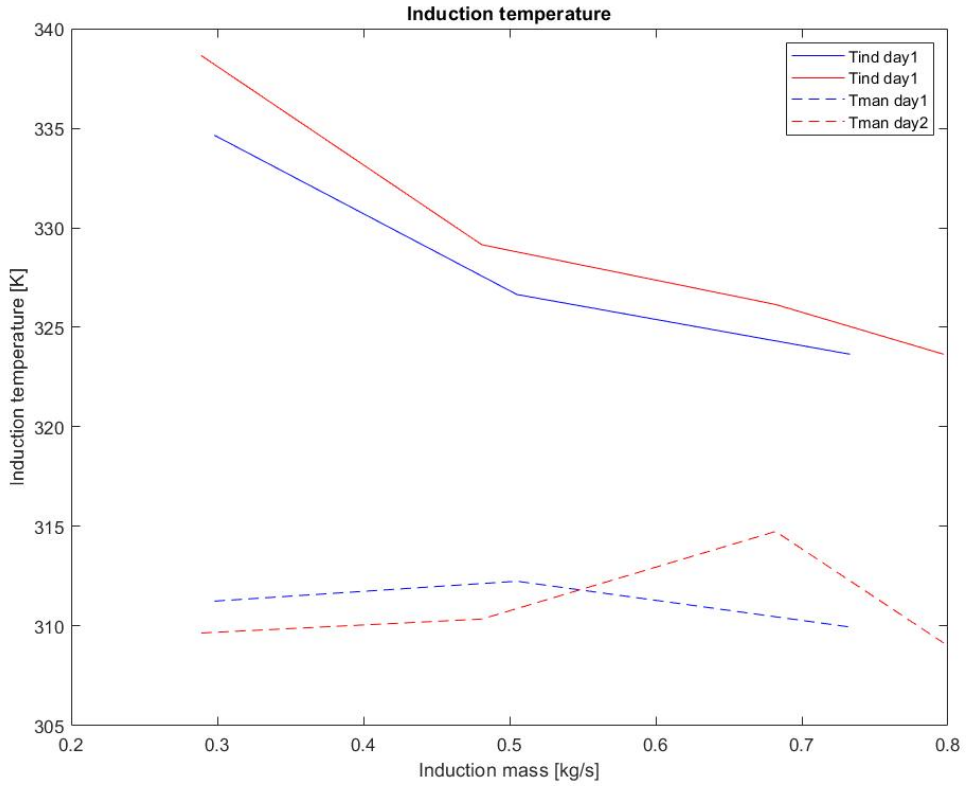

Figure 4.1: Induction temperature and inlet manifold temperature versus induction mass

In figure 4.1, the induction temperature and inlet manifold temperature is plotted against the induction mass for the two test days. It is clear that the induction temperature is higher than the inlet manifold temperature. This is due to the heat generated form the cylinder. The casing of the inlet manifold close to the hot cylinder heats up. Thus, when the mixtures passes the warm casing of the inlet manifold the mixture will heat up as well.

An other visible effect is that, the induction temperature decreases with an increase in induction mass flow. An increase in induction mass also means an increase in power. One would think that with an increase in power the temperatures would rise instead of drop. Namely, with an increase in power the cylinder temperature rises. Thus, the manifold casing temperature rises and thereby also the heat pick-up. But, this effect is countered by the decrease in exposure time. Since, the induction mass flow increases, the time the mixture is exposed to the hot manifold casing decreases. Meaning, less heat can be transferred. Thus, it has a lower induction temperature.

A note should be made that, the temperature of the casing of the inlet manifold was not measured. Thus, the claim that the casing temperature increases with an increase in power could not be proven. But, it is a reasonable assumption. The amount the casing temperature increases would be an interesting subject for future research.

4.3. Pressure difference over inlet valve

In the chapter above, the temperature difference of the inlet manifold and the trapped temperature is investigated. The same investigation can be done for the pressure. To investigate this, the inlet manifold pressure and the trapped pressure need to be compared. The inlet manifold pressure is measured during the two test days. But, accurate in-cylinder measurements could not yet be obtained. To still investigate this effect, data from Sapra [16] is used. He performed elaborate tests in 2017, where the inlet manifold pressure and the in-cylinder pressure were measured for the same engine.

Figures 4.2, 4.3 and 4.4 show examples of the p-v diagram of the induction process for 450kW, 374kW and 250kW. The figures also depict the corresponding inlet manifold pressure and valve timing. Where, IVC is inlet valve closing, IVO is inlet vale opening, EVC is the exit valve closing and EVO is exit valve opening. With this data the pressure difference of the inlet manifold to the cylinder at trapped conditions (IVC) can be calculated. In figure 4.5 boxplots show the pressure difference of all the tests Sapra performed for the corresponding power.

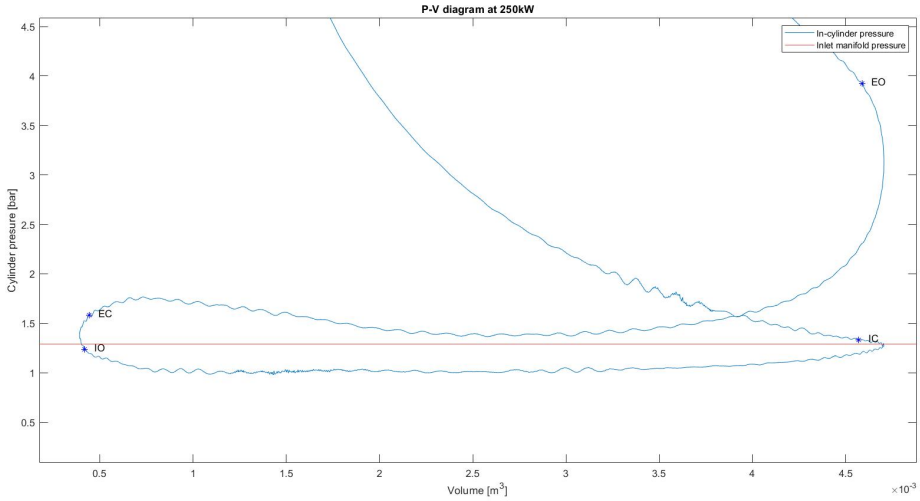

Figure 4.2: Measured P-V diagram at 250 kW

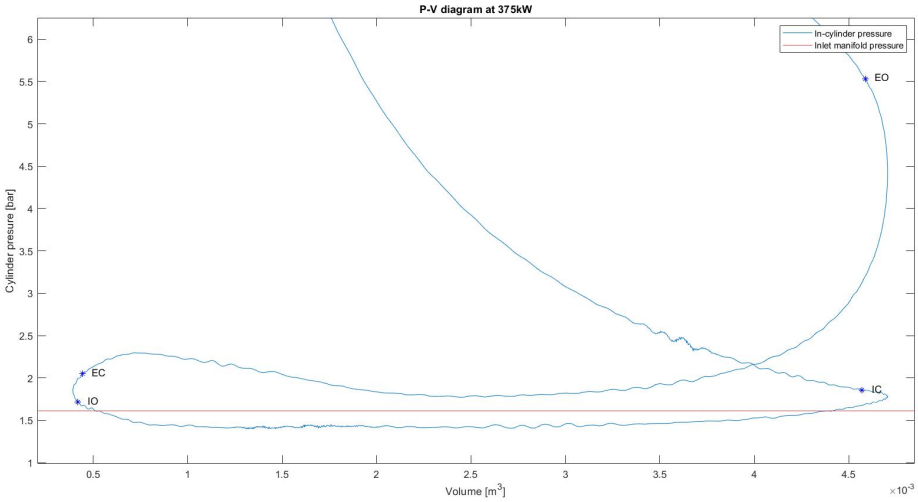

Figure 4.3: Measured P-V diagram at 375 kW

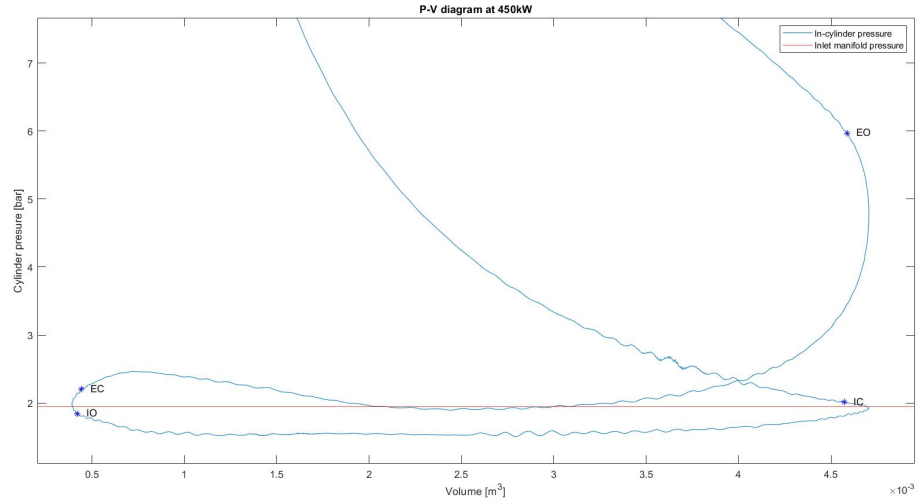

Figure 4.4: Measured P-V diagram at 450 kW

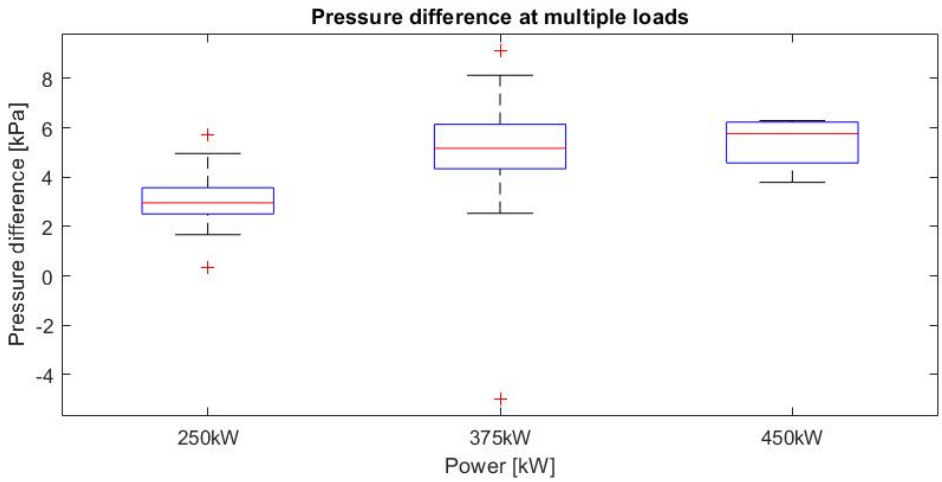

Figure 4.5: Box plot of pressure difference between MAP and P1 at multiple loads

The first thing that can be noticed is that, the pressure of the trapped condition is higher then the pressure in the manifold. This could be explained by the ramming effect. As explained in chapter 3.1.2, the ramming effect causes an increase in pressure when the cylinder slows down or reverses during the induction process due to the inertia of the gas. Another effect explained in chapter 3.1.2 is the friction loss effect. The friction loss effect states that the pressure drops when there is an obstruction. Since, the inlet valve is an obstruction, the inlet valve would cause a pressure drop from the inlet manifold to the in-cylinder trapped pressure. But, this effect is apparently countered by the ramming effect.

The second thing that can be noticed is that, the pressure difference increases with an increasing power. This can be explained by the fact that, the ramming effect increases at higher loads. Because, at higher loads the inlet flow is higher. Thus, also the inertia of the gas is higher, due to the charge pressure.

A note should be made on the accuracy of the measurements.

First of all, the pressure sensor only has an accuracy of 1.25 bar, as can be seen in table 2.2. The sensor was installed to investigate the combustion process, since during the combustion there are high pressure with large differences. But now, we look at the induction stroke with low pressures and differences between valve timings of only one bar. So, the pressure sensor does not have the required accuracy to investigate this effect.

Secondly, the valve timings were not measured during our experiments. They were taken from the paper of Sapra [15]. He stated that the engine has no valve overlap. But, after exhaust valve closed, the pressure still decreases even though all the valves are closed and the volume decreases. Looking at the P-V diagrams, it would be more logical that there is valve overlap. This could be explained by the inaccurate pressure sensor at low pressures or by incorrect valve timings. Thus, we do not only have doubts about the pressure sensor accuracy, but also about the valve timings.

5

Volumetric efficiency model

In this chapter the effects discussed in chapters 4.2 and 4.3 will be used to improve the prediction of the volumetric efficiency of the state of the art model discussed in chapter 3.2.1. The model will than be compared with the original model and the experimental based volumetric efficiency calculation described in chapter 4.1.

5.1. Improved 0-dimensional model

This chapter discusses improvements on the state of the art model, to better calculate the volumetric efficiency . This will be done by incorporating the effects discussed in chapter 4. A note should be made that, the parameters are compared to the inlet manifold mass flow and not the power. This is because, the inducted temperature is a function of the inlet manifold mass flow. The output power calculated by the model at these mass flows is higher than the measured power, as can be seen in table 5.1 .

This could be caused by the tuning of the engine model. The Seiliger parameters, which determine the in-cylinder conditions, were calculated by measurements performed on the engine in 2019 [16]. Since then, some parts of the engine where swapped out. This could cause different Seiliger parameters. And Moreover, the dutch gas net supplies the engine from natural gas. In the past its main source was from Gronningen. Now, the gas originates from abroad. The different composition of the gas from abroad could have a significant effect on the in-cylinder conditions. Thus, if the full function of the model would be used, the in-cylinder Seiliger parameters should be tuned again on the current conditions. But, for this research this is not necessary. The focus lies on the induction process.

Table 5.1: inducted mass and power comparison

Name	Unit	Condition 1	Condition 2	Condition 3	condition 4
Measured inducted mass	kg/s	0.297	0.493	0.701	0.818
Measured power	kW	116	245	364	417
Original model inducted mass	kg/s	0.298	0.491	0.704	0.816
Original model power	kW	123	265	422	470
Improved model inducted mass	kg/s	0.295	0.496	0.705	0.818
Improved model power	kW	139	284	433	480

5.1.1. Induced temperature

As described in chapter 4.2, the inducted mass mixture rises in temperature from the inlet manifold thru the inlet runner to the cylinder. It starts at a temperature from around 35°C (308.15K), regulated by the inter-cooler, and rises to around 52°C-67°C (325K-340K) before entering the cylinder. This is due to the hot inlet runner casing. The hot inlet runner casing heats up the mixture when it flows through the inlet runner. At a higher power more air and fuel passes through the inlet runner with the same heat pick up. This means the temperature of the mixture at high power will be lower, since the same heat pick-up needs to warm up more mass. This effect is depicted in figure 5.1, where the full line depicts

the manifold temperature and the green dotted line the measured inducted temperature.

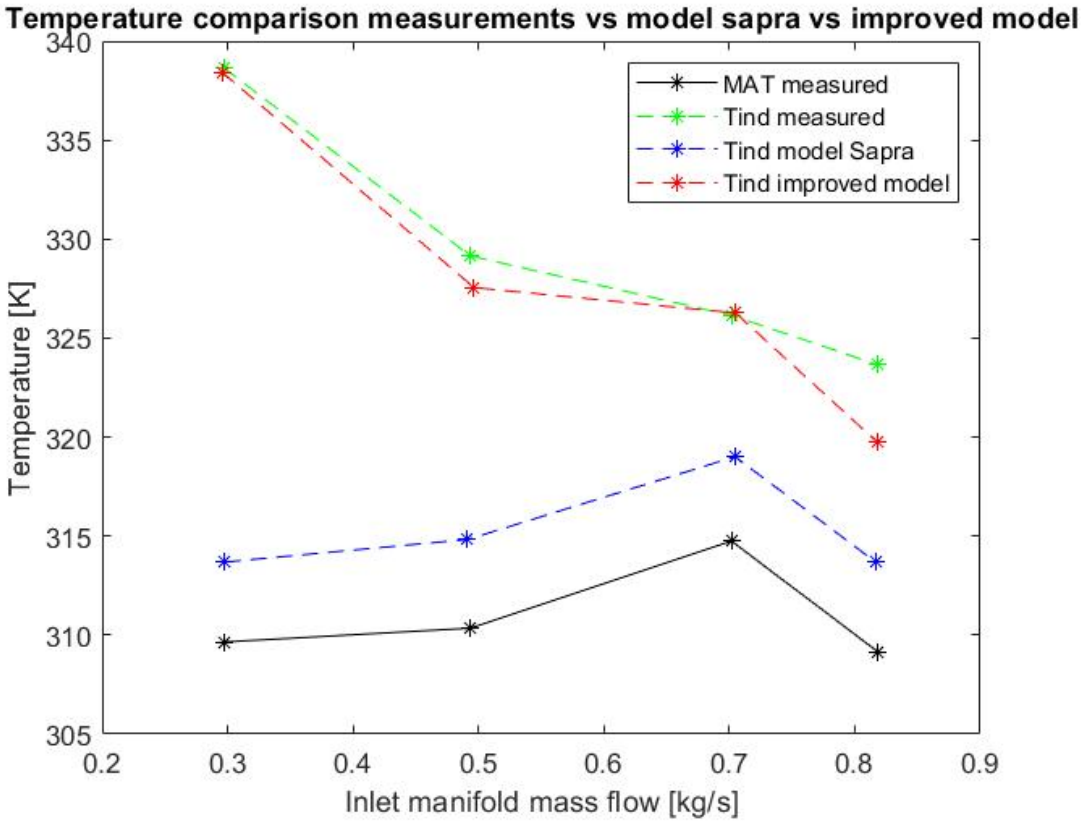

Figure 5.1: inducted temperature comparison of measurements, original model and improved model.

In the original model the induced temperature is calculated by formula 5.1. Where, ϵ_{inl} is the heat exchange effectiveness, equal to 0.05 and T_{inl} is the inlet wall temperature, equal to 400K. In figure 5.1, this is depicted by the blue dotted line. As can be seen, is the prediction of the original model significantly lower than the measured values. Moreover, the effect of decreasing temperature at increasing mass flow is not visible. The formula used in the original model does not include any mass flows.

$$T_{ind} = \epsilon_{inl} \cdot T_{inl} + (1 - \epsilon_{inl}) \cdot T_{iman} \tag{5.1}$$

To improve the original model, a new equation for the induction temperature will be created. This equation will include the mass flow effect and increases the heat exchange. This results in an estimation closer to the measured results.

The new equation is determined as follows. Consider the inlet runner, that heats up the induction mass, a heat exchanger. In an extreme case the induction mass would reach the inlet runner temperature. But, in general it stays much lower. This effect can be described by the heat exchange effectiveness. The heat exchange effectiveness of a heat exchanger is defined as the ratio of the actual heat transfer over the maximum heat transfer possible. The definition is described in equation 5.2. Where $\epsilon_{inl-new}$ is the new heat exchange effectiveness of the inlet runner, Q_{actual} is the actual heat transfer and Q_{max} is the maximum possible heat transfer.

$$\epsilon_{inl-new} = \frac{Q_{actual}}{Q_{max}} \tag{5.2}$$

The actual heat transfer is the heat transfer needed to heat up the induction mass from the inlet manifold temperature to the induction temperature. This is calculated by equation 5.3. Where, c_p is the specif heat at constant volume of the mixture and $T_{ind-new}$ the new induced temperature.

$$Q_{actual} = m_{in} \cdot c_p \cdot (T_{ind-new} - T_{iman}) \tag{5.3}$$

The maximum heat transfer is either, the heat transfer to heat up the mixture to the inlet runner wall, or the heat transfer the inlet runner wall can dissipate. The maximum heat transfer of the induced mixture is given by equation 5.4. Where $Q_{max-mix}$ is the heat transfer of the induced mixture. Equation 5.5 gives the maximum heat transfer of the inlet runner. Where $Q_{max-runner}$ is the heat transfer of the inlet runner and C_{iman} the heat constant of the inlet runner wall.

$$Q_{max-mix} = c_p \cdot m_{in} \cdot (T_{inl} - T_{iman}) \tag{5.4}$$

$$Q_{max-runner} = C_{iman} \cdot (T_{inl} - T_{iman}) \tag{5.5}$$

The maximum of the two is the maximum heat transfer possible. But, if the heat transfer of the mixture is chosen, c_p and m_in would cancel out in equation 5.2 with equation 5.3. Therefore, the maximum heat transfer of the inlet runner wall will be used in the new heat exchange effectiveness equation. This means that theoretically the heat exchange effectiveness could be higher than one. Now, with the maximum heat transfer of the inlet runner wall as the maximum heat transfer, the new heat exchange effectiveness of equation 5.2 becomes equation 5.6.

$$\epsilon_{inl-new} = \frac{m_{in} \cdot c_p \cdot (T_{ind-new} - T_{iman})}{C_{iman} \cdot (T_{inl} - T_{iman})} \tag{5.6}$$

Rewriting this to the induction temperature gives equation 5.7. In this new equation the effect of the induction mass flow is now taken into account.

$$T_{ind-new} = \frac{\epsilon_{inl} \cdot C_{iman} \cdot (T_{inl} - T_{iman})}{m_{in} \cdot c_p} + T_{iman} \tag{5.7}$$

The variables in equation 5.7 are determined as follows. The specific heat at constant pressure(c_p) is a property of the inducted mass and equal to 1.1 kJ/(kgK). The manifold wall temperature (T_{inl}) was not measured during the experiment. But, Sapra estimated it to be be 400K. In this research the same value will be used. The heat capacity of the inlet runner is 1.1 kJ/(K). It is the product of the specific heat of steel (0.42 kJ/(kgK)) and the mass of the inlet runner (2.61 kg). The new heat exchange effectiveness is 0.095. It is not directly measured, but tuned by using the induced temperature measurement data. Now with the new induced temperature equation, the induced temperature better resembles the measured induced temperature. Figure 5.1 shows the results of this improvement.

5.1.2. Manifold pressure

As described in chapter 4.3, the trapped pressure is higher than the inlet manifold pressure. In the state of the art model, discussed in chapter 3.2.1, the trapped pressure is assumed to be equal to the manifold pressure. Thus, to improve the volumetric efficiency an equation should be added to take into account this pressure increase. But, with the limited data and the multiple effect that cause the pressure difference, no equation based on physics could be found. Instead the average pressure difference ($p_1 - p_{man}$) per operating point, determined in chapter 4.3, are used in the model. Table 5.2 shows these values. The effect of the pressure difference on the volumetric efficiency is discussed in chapter 5.2.

Table 5.2: Difference inlet manifold pressure and trapped pressure

Name	Unit	Condition1	Condition 2	Condition 3	condition 4
Pressure difference	Pa	-771	2960	4900	5300

5.1.3. Residual mass

Now, the volumetric efficiency of the model with improved pressure and temperature is plotted together with the measured volumetric efficiency and the volumetric efficiency calculated with the original model (figure5.2). In the figure it is visible that the volumetric efficiency estimation of the improved model has a better trend than the original model. It increases instead of decreases with increasing mass flow.

But, in general the volumetric efficiency of the improved model has a bigger deficit to the measured volumetric efficiency. It lies about 10% lower than the measured volumetric efficiency. The volumetric efficiency of the original model has a 9% deficit at high mass flows. At low mass flows the deficit is only 2%.

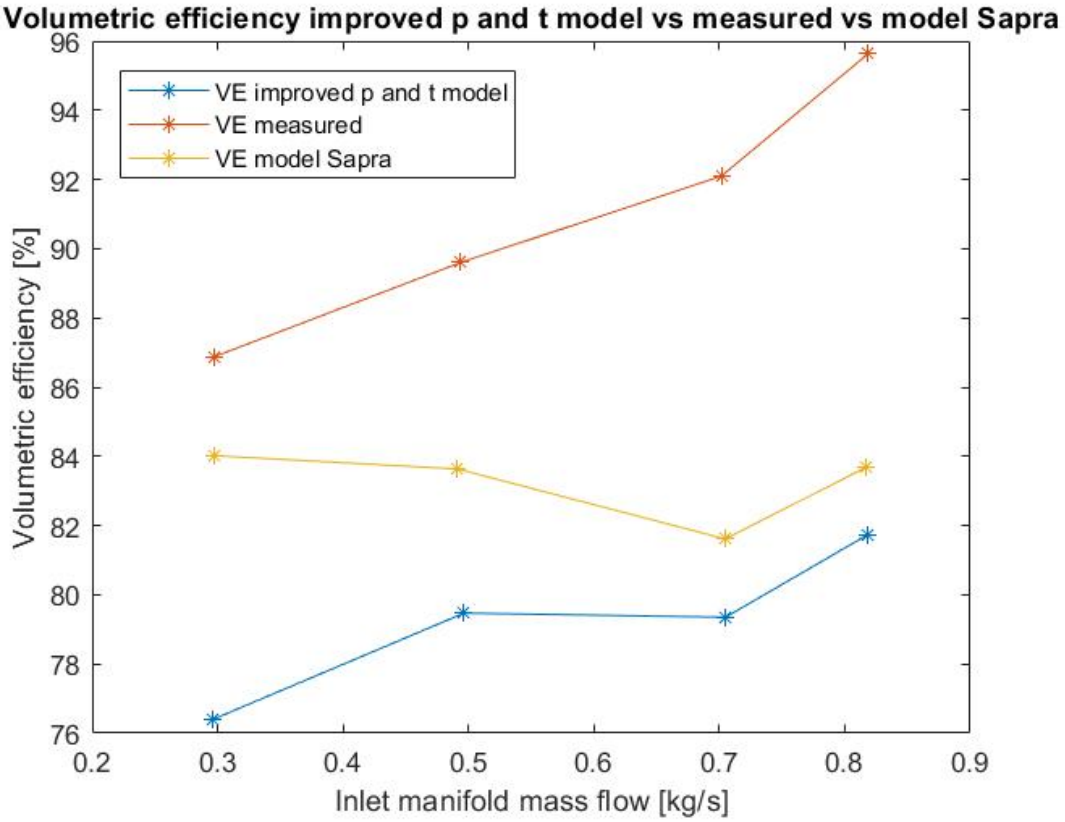

Figure 5.2: Volumetric efficiency of pressure and temperature improved model, measurements and original model

The explanation for the deficit of 10% lies in the initial estimation of the residual mass. In the models the residual mass is estimated by first estimating the initial manifold pressure by equation 3.10. Then, the manifold pressure is used to calculated the trapped mass with the ideal gas law (equation 3.11). And finally, the residual mass is determined by subtracting the air mass and fuel mass of the trapped mass. The air mass and fuel mass in this equation are calculated by parametric equations. With this residual mass estimation the residual mass is estimated too high. The residual mass takes in space that otherwise would be filled with inlet manifold mass. Meaning that, the volumetric efficiency is estimated too low.

The solution for this is a different initial residual mass estimation. Ideally, the residual mass is calculated with the ideal gas formula at exit valve closed (EVC) . At EVC, all the mass that remains in the cylinder is the residual mass. But, the pressure and temperature at EVC are not known yet. To know these values first the combustion process needs to be simulated.

Instead, the ideal gas law is used at inlet valve closed (IVC). The method assumes that the following masses occupy the following volumes. First, The trapped mass (m_1) is the total mass in the cylinder at IVC. It occupies the whole cylinder volume, when the inlet valve closes (V_{IVC}). Secondly, The induced mass (m_{ind}) is all the fuel and air inducted into the cylinder during the induction process. It occupies the induced volume (V_{ind}). The induced volume is the volume between inlet valve open (IVO) and IVC (equation 5.8). During these two points in time, the inlet valve is open and mass can be inducted . Finally, the residual mass (m_{res}) is the mass still present from the previous combustion cycle. It occupies the volume that is not occupied by the induced mass at IVC. This is for this method assumed as the volume at inlet valve opening (V_{IVO}). All the discussed masses and volumes can be found in figure 5.3.

$$V_{ind} = V_{IC} - V_{IO} \tag{5.8}$$

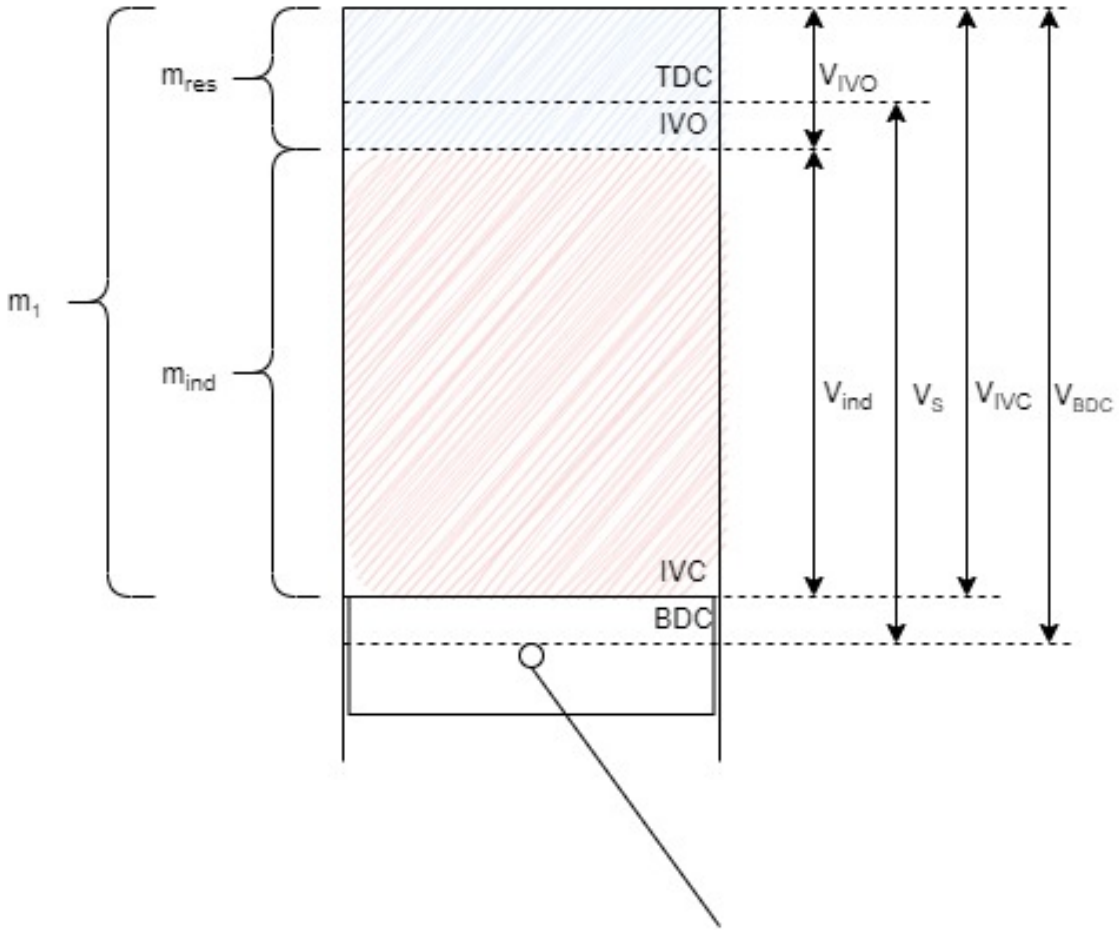

Figure 5.3: Cylinder volume and masses assumptions for the new residual mass method

With the above assumptions about the masses and volumes, the residual mass can be calculated by using the following formulas. First, the induced mass is calculated by parametric equations as explained in chapter 3.2.1. Two of the combustion parameters he investigated were the fuel and air mass input. These two mass flows combined is the induced mass.

Next, with the assumption that the induced mass occupies the induced volume at IVC, the new initial trapped pressure is calculated with the ideal gas law as in equation 5.9. Where $p_{initial-1-new}$ is the new initial trapped pressure, R_{im} is the gas constant of the fuel and air mixture and $T_{initial-1}$ is the initial trapped temperature. The initial trapped temperature is estimated at 440K for every load. In reality the temperature changes depending on the load. But, this effect is not yet included in thee initial calculations. In future work this could be included in the parametric equations.

$$p_{initial-1-new} = \frac{(m_{ind}) \cdot R_{im} \cdot T_{initial-1}}{V_{ind}} \tag{5.9}$$

Finally, the new residual mass ($m_{initial-res-new}$) is calculated with the new initial trapped pressure over the remaining volume (V_{IVC}) in equation 5.10. The gas constant of the residual mass is assumed the same as the gas constant of the inducted mass.

$$m_{initial-res-new} = \frac{p_{initial-1-new} \cdot V_{IVO}}{R_{im} \cdot T_{initial-1}} \tag{5.10}$$

With this new initial residual mass calculation implemented in the improved model, the volumetric efficiency rises with about 10%. The new improved model now predicts the volumetric efficiency with greater accuracy, as can be seen in figure 5.4.

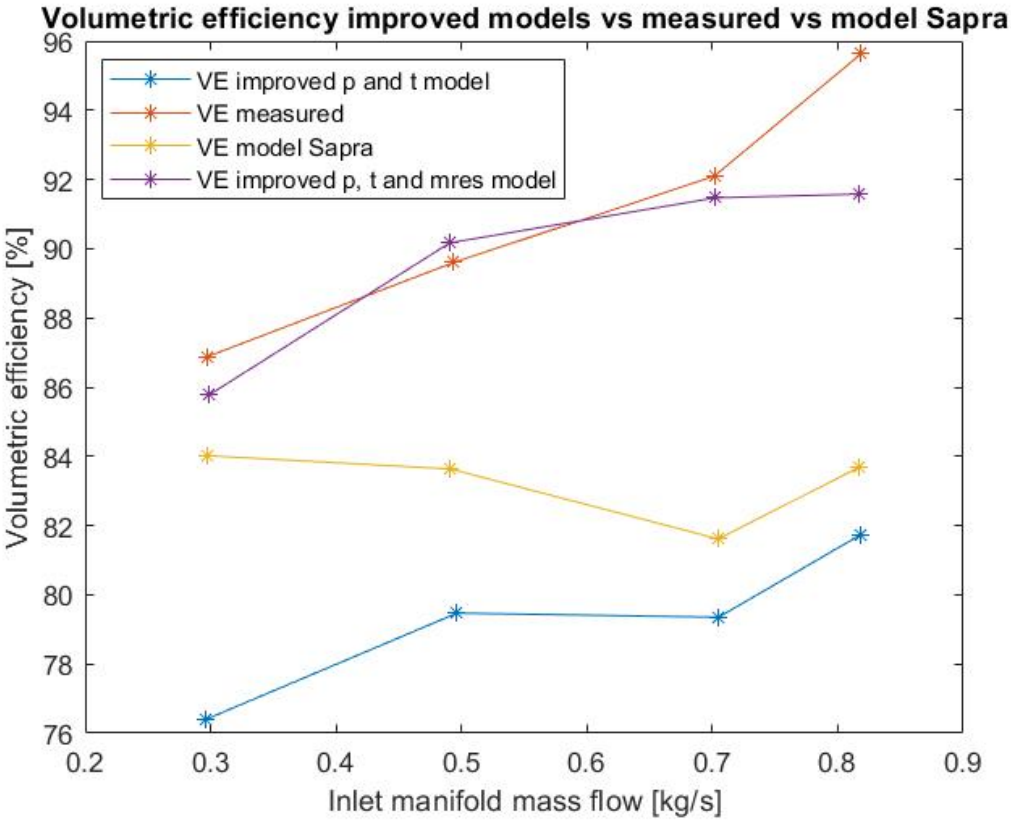

Figure 5.4: Volumetric efficiency of improved models, measurements and the original model

5.2. Analyses improved model

In this chapter the effect of the improvements of the model, as discussed in the chapter above, on the volumetric efficiency will be discussed. The improvements will be compared to the original model [15] and the measurements. The volumetric efficiency is not directly measured, but as discussed in chapter 4.1, calculated using the O2 percentage in the exhaust gas.

5.2.1. Improvements to the original model

In this chapter the effects of the improvements made to the original model [15] will be discussed. First, the effect of the new induced temperature is discussed. Then, the effect of the addition of the pressure difference between the manifold pressure and trapped pressure is discussed. Finally, the effect of the new residual mass calculation are discussed.

Induced temperature effect

First, the effect of the new induced temperature on the original model [15] will be discussed. In figure 5.5 the volumetric efficiency is plotted against the inlet manifold mass flow. The orange line in the figure is the volumetric efficiency of the original model. The yellow line is the volumetric efficiency of the original model with the new induced temperature. The blue line is the measured induced temperature.

The new induced temperature formula has two effects on the volumetric efficiency. The first effects is a general lower volumetric efficiency compared to the original model. Compared to the measured volumetric efficiency this is an deterioration. But, the other effect is that the volumetric efficiency increases with increasing mass flow instead of a decrease. Compared to the measured volumetric efficiency this is an improvement. The measurements show a clear increase in volumetric efficiency with increasing

mass flow. To conclude, the new induced temperature formula produces lower and thus worse volume efficiency predictions. but, the trend of the volumetric efficiency is predicted better.

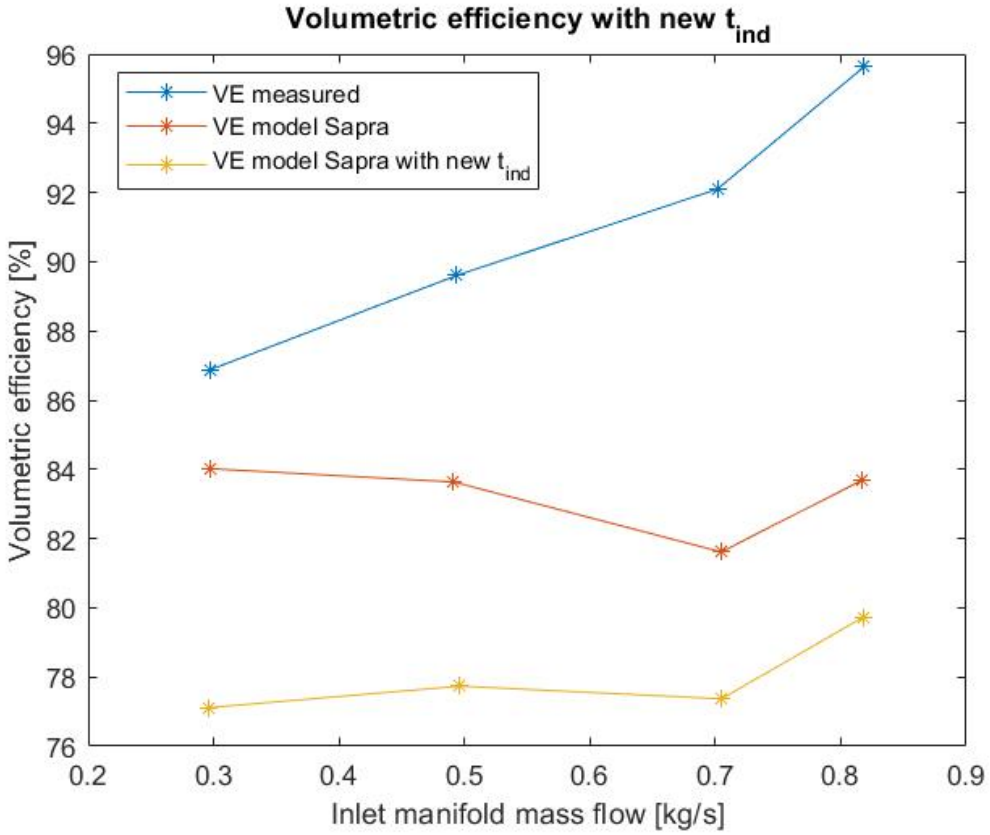

Figure 5.5: Effect Tind formula on volumetric efficiency

Pressure difference effect

Secondly, the effect of the new pressure difference is added to the original model. In figure 5.6 the effect of the pressure difference of the manifold pressure and trapped pressure on the volumetric efficiency is added. The purple line depicts the volumetric efficiency of the original model with the new induced temperature and the new pressure difference.

The effect of the pressure difference is that in general the volumetric efficiency increases. Only for the mass flow of 0.3 kg/s the volumetric efficiency decreases. one could also say that, the volumetric efficiency increases more with increasing mass flow. This would be an improvement compared to the measurements. But, for making this assumption more measuring points are needed. To conclude, the addition of the pressure difference has a positive effect on the volumetric efficiency prediction compared to the original model.

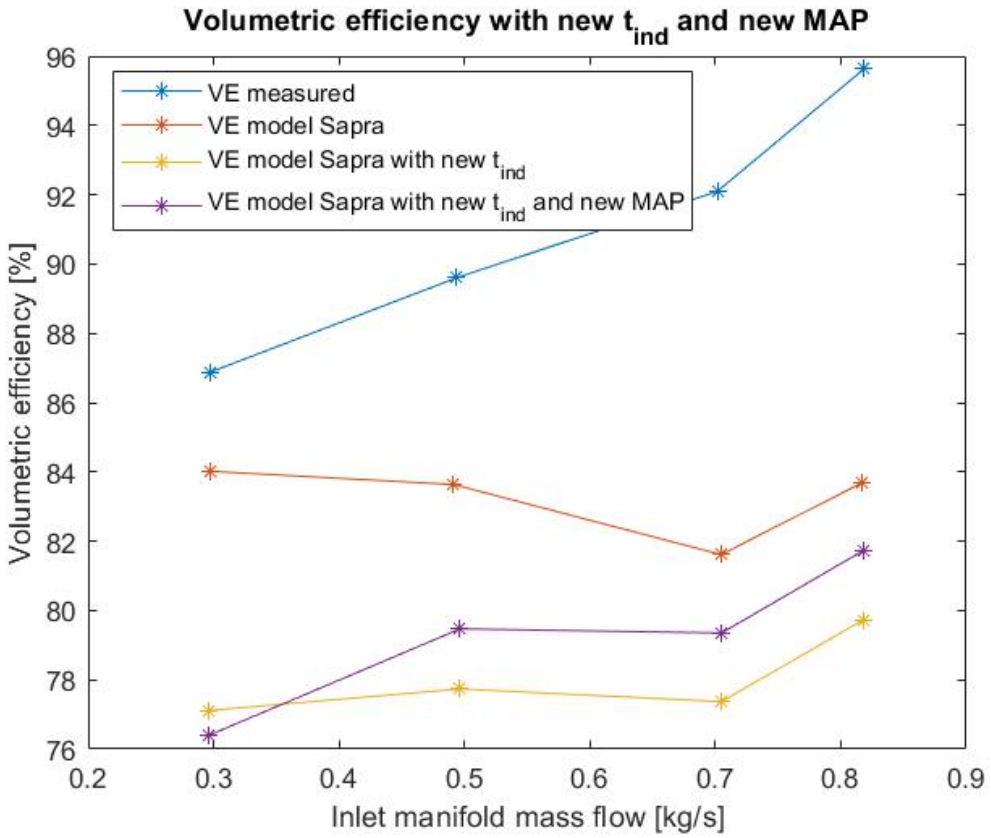

Figure 5.6: Effect pressure difference on volumetric efficiency

Residual mass effect

Finally, the new residual mass effect is added to the volumetric efficiency model. In figure 5.7 the green line depicts the volumetric efficiency with all the effect are added to the volumetric efficiency.

The addition of the new residual mass calculation has the largest effect of all effects. It significantly increases the volumetric efficiency. With this increase the model predicts the volumetric efficiency similar to the measured volumetric efficiency.

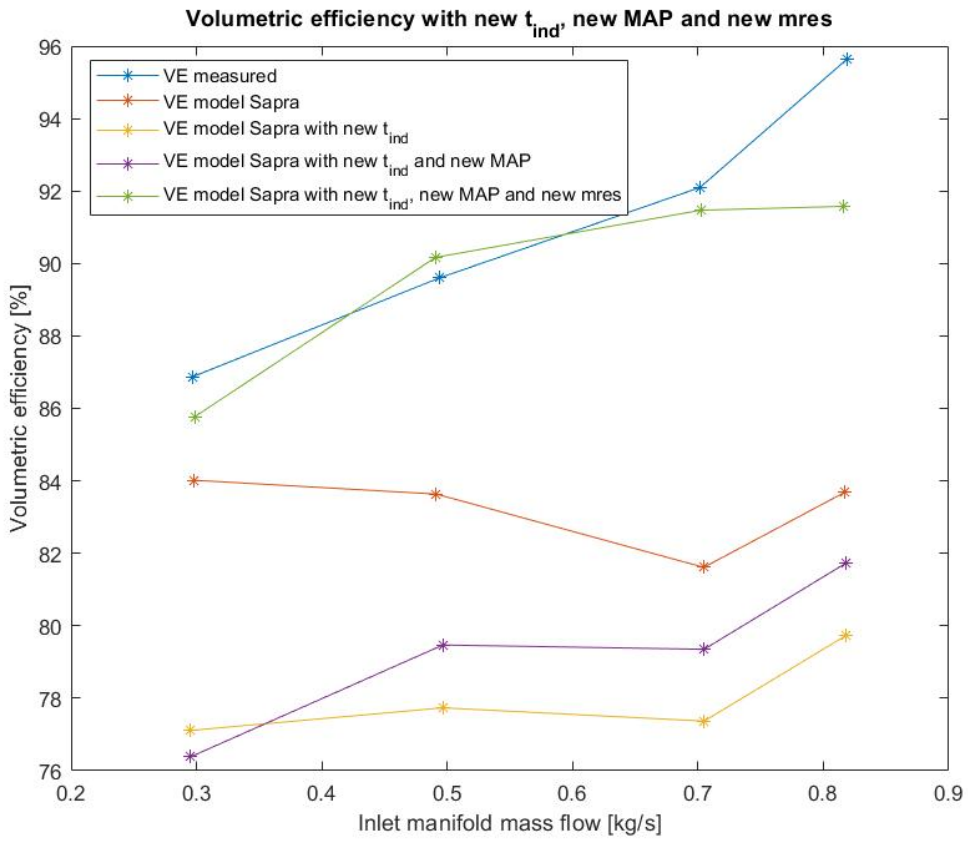

Figure 5.7: Effect pressure difference on volumetric efficiency

5.2.2. Volumetric efficiency breakdown

Ideally, the volumetric efficiency is 100%. This would mean that no losses occur between the manifold and the cylinder. Unfortunately, this is not the case. In chapter 3.1.2, most of the effects that contribute to less mass inducted into the cylinder are discussed. During this research it was not possible to model all these losses, but three losses were modelled.

Firstly, there is less mass inducted into the cylinder due to a temperature increase from the inlet manifold to the cylinder. Due to the temperature increase the density decreases. Thus, less mass is inducted into the cylinder. This volumetric efficiency decrease is about 12% for low mass flows and 10% for high mass flows. This is visible by the orange line in figure 5.8.

Secondly, a difference in mass induction is present due to a pressure difference between the manifold and cylinder. The pressure once again affects the density of the mixture. At higher pressures the density increases. Thus, there is more mixture present. The effect of the pressure difference for this engine is that, at low mass flows the volumetric efficiency decreases with about 1%, and at high mass flows the volumetric efficiency increases with about 3%. This is visible by the yellow line in figure 5.8. The first decrease and then increase of the volumetric is due to the ramming effect. This is elaborately explained in chapter 4.3.

Lastly, the presence of residual mass effects the volumetric efficiency. If, residual mass is present in the cylinder, it takes in space that otherwise would be filled by the induction mass. Thus, if more residual mass is present the volumetric efficiency will decrease. The effect of residual mass present in the cylinder is a decrease of about 2%. This is visible by the purple line in figure 5.8.

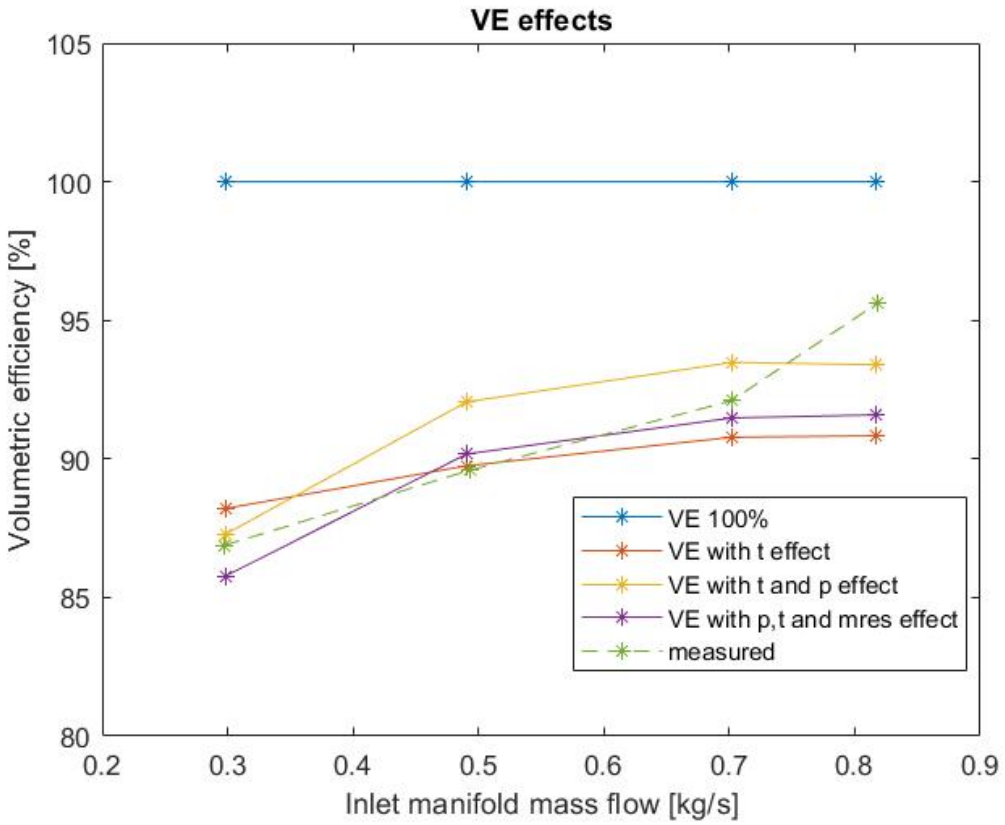

Figure 5.8: Effect on the volumetric efficiency

The conclusion is that by only modeling the temperature pressure and residual mass effect, the volumetric efficiency can be estimated with a maximum error of 4%. This error is only for high mass flows. At lower mass flows the error is lower than 1%.

6

Conclusions and recommendations

This chapter will provide the conclusions and recommendations for this thesis work and future volumetric efficiency modeling work.

6.1. Conclusions

This report was written to answer following main research question: ”How can the estimation of the volumetric efficiency be improved of state of the art 0-dimensional spark ignited gas engine models?” The underlying goal of this research was to get a better understanding of the starting conditions of the combustion process, which is crucially important to accurately predict performance parameters such as efficiency and CO_2 and NO_x emissions. The parameter used in this thesis to describe all starting conditions of the combustion process is the volumetric efficiency. The acquired knowledge on the starting conditions can then be used to further develop the 0-dimensional model of the Caterpillar G3508 gas engine.

First, the definition of the volumetric efficiency was further clarified. The volumetric efficiency is a dimensionless measure to evaluate the induction of a four stroke engine as a gas pumping device. But, authors use many different variations of the definition. There is no clear definition that is universally. In general the volumetric efficiency is the fraction of the actual mass inducted into the cylinder and a theoretical mass that at ideal circumstances could be inducted into the cylinder. The absolute value of the volumetric efficiency is often not as important as the ability to compare the volumetric efficiency at different speeds, loads or engines. Therefore, the most import thing is to be consistent in the definition when using the volumetric efficiency. Since, this thesis uses a turbocharged engine, where the natural gas and air are mixed before the turbocharger, the manifold conditions will be used for the theoretical induced mass and the sum of air mass and fuel mass will be used for the actual induced mass.

Secondly, this research lists the main effects that could influence the volumetric efficiency of the caterpillar G3508 engine. Six effects were found: The air fuel ratio, heat transfer, residual mass, valve timing, friction losses and the turbocharger.

The effect of the turbocharger is that it creates a higher pressure. The higher pressure then creates more actual mass inducted. This higher pressure is created before the inlet manifold. Thus, has no effect on the volumetric efficiency definition used in this thesis.

The friction loss effect is the effect of pressure loss between the manifold and cylinder. The pressure influences the density of the mass. This also influences the volumetric efficiency. This effect is partially implemented in the improved model.

The valve timing can have multiple effects. Firstly, it controls the valve overlap. If there is valve overlap, scavenging occurs. This influences the amount of residual mass present in the cylinder. Sapra [15] claimed that there is no valve overlap on the the engine thus this effect does not occur on this engine. But, P-V measurements showed that during the induction stroke the pressure dropped even though all the valves were closed and the volume decreases. This observation can either be explained by a measurement inaccuracy. namely, the pressure sensor has an accuracy of 1.25 bar. It is build for high

pressure measurements during the combustion process with large differences, not for low pressure measurements during the induction stroke with small differences. Or by the assumption that the valves do overlap. This should be investigated in the future. Secondly, the valve timing influences the timing of inlet valve closing. If, the inlet valve closes after bottom dead center, back flow or ramming could occur. Back flow is the effect of mass pushed back to the inlet manifold due to the decreasing volume of the cylinder. Ramming is the effect of mass still entering the cylinder even if the cylinder volume decreases. This is due to the high inertia of the induced mass. The ramming effect and back flow effect are partially implemented in the improved model.

The residual mass effects the volumetric efficiency by occupying space that would otherwise be used by the induced mass. This effect is implemented in the improved model.

The heat transfer effect is the effect of increasing temperature from the manifold to the cylinder. The temperature influences the density of the mass thus also the volumetric efficiency.This effect is implemented in the improved model.

The last effect is the air fuel ratio effect. The air fuel ratio regulates the composition of the induced mass. The composition of the mass has an effect on the actual induced mass. Especially when only air or fuel is needed for the actual induced mass. This effect is not implemented in the improved model.

After the research on the definition of the volumetric efficiency and the theoretical effects on the volumetric efficiency, test were performed on the Caterpillar G3508 engine. The tests were performed for 2 reasons: to measure the volumetric efficiency and to investigate some effects, which are important for the volumetric efficiency. These effects are then incorporated into the original model [15].

The volumetric efficiency could not be measured directly. To measure the volumetric efficiency the actual flow into the cylinder needs to be measured. But, the engine was only equipped with a flow meter for the natural gas. To overcome this problem we have established the volumetric efficiency by calculating the air mass flow from the amount of oxygen in the exhaust as proposed in Stapersma [19]. As the calculation in Stapersma [19] was for a diesel engine and neglected the effect of NOx emissions, we adapted this method for a natural gas engine, by using the composition of natural gas and adding the effect of NOx emissions. Thus, this thesis describes how the method for diesel engines is adapted to work for natural gas engines.

The other reason why test were performed was to investigate some effects which are important for the volumetric efficiency. First, temperature measurements were performed to investigate the temperature rise of the induced mixture form the manifold to the cylinder. This rise is due to the hot inlet runner that connects the manifold to the cylinder. The wall of the inlet runner heats up the induced mixture by convection. in the original model the temperature is constant over the whole power range. But, the tests concluded that with increasing power the temperature decreases. This is because at higher power more mass is inducted into the cylinder. Meaning, with the same amount of heat added to the mixture, the mixture increases less in temperature. To incorporate this effect into the model, a new formula for the heat exchange effectiveness is created which includes the induced mass flow.

The second effect that was investigated is the change in pressure from the manifold to the cylinder. The goal was to measure the pressure in the cylinder and manifold. But, no accurate measurements could be obtained inside the cylinder. The correct sensors were not installed yet. For this research the in-cylinder pressure measurements of Sapra [15] are used. He did excessive measurements on the in-cylinder pressure and manifold pressure on the same engine in the past. Out of these measurements the conclusion is that at low mass flows the pressure drops from the manifold to the cylinder. This is due to the friction losses over the inlet valve and due to the fact that the volume already decreases before the inlet valve closes. But, at higher mass flows the pressure rises from the manifold to the cylinder. The cause given in this thesis is the ramming effect. At high mass flows the inertia of the induced mixture is high. This means that even though the cylinder volume decreases, mass still flows into the cylinder. This creates higher pressure in the cylinder. For the temperature rise a formula based on the convection of heat could be made. But, the pressure difference is effected by multiple effect. So, no such formula could be created. Instead, a table with the measured difference were added to the model.

The last effect that was investigated is the residual mass effect. The residual mass takes in space that otherwise would be used by the induced mass. But, the original model [15] estimates the residual

mass to high. In the improved model the residual mass is calculated based on the in-cylinder conditions instead of the manifold conditions. This improves the volumetric efficiency predictions by 10%.

With all the new effect added to the model original model [15], an improved model is created. This improved model predicts the volumetric efficiency with a 4% accuracy at high power and mass flows, and with 1% accuracy at average and low loads and mass flows. This is a large improvement compared to the original model [15]. It predicts the volume efficiency 3% lower at low loads and mass flows, and 12% lower at high loads and mass flows.

6.2. Recommendations

I have the following recommendations to improve this work and for further research projects.

- For the formula of the induced temperature the wall temperature of the inlet runner was estimated and held constant. In reality, i expect it to rise in temperature with increasing power. At higher power more heat is created in the cylinder. This would heat up the cylinder more. I expect that the environment also plays a role in the temperature of the inlet runner. In future research the inlet runner wall temperature should be investigated. I expect that a relation can be found between the engine power, environmental conditions and inlet runner wall temperature.
- During the test days, the induced temperature at every cylinder was measured. But, only the minimum and maximum temperature were saved. This research uses the average to determine the induced temperature. In future research the induced temperature at every cylinder should be saved and studied.
- In this research no formula to calculated the pressure difference between the manifold and cylinder could be found. In future research to focus could lie on investigating all the effect that cause this pressure difference. This could be done by for example CFD simulation of the induction process.
- This research assumes that no scavenging takes place. But, the PV diagrams shows that the pressure drops when all the valves are closed and the volume decreases. This observation can either be explained by a measurement inaccuracy. namely, the pressure sensor has an accuracy of 1.25 bar. It is build for high pressure measurements during the combustion process with large differences, not for low pressure measurements during the induction stroke with small differences. Or by the assumption that the valves do overlap. Therefore, i recommend to perform new measurements on the valve timing and to use a pressure sensor with a smaller uncertainty at low pressures.
- The in-cylinder parameters of the engine model are not tuned in this research. This means that the power predictions of the model were not the same as the measured power. To make the improved model complete, new test should be performed to tune the in-cylinder parameters.
- The formula for the induced temperature uses the manifold temperature as one of the parameters. But, measurements were only performed with the manifold temperature ranging from 35°C to 42°C. In future research the induced temperature should be investigated at a wider range of manifold temperatures. This is especially important for the evaporation of methanol in the manifold.

Bibliography

[1] Bengtsson. *Modelling of Volumetric E±ciency on a Diesel Engine with Variable Geometry Turbine*. 2002.

[2] Bosklopper. *Experimental and simulation based investigation of the performance of a 100% methanol port injected spark-ignited engine*. 2020.

[3] J Ellis and K Tanneberger. *Study on ethyl/methyl alcohols for shipping*. 2015.

[4] European comission". *Reducing emissions from the shipping sector*. Feb. 16, 2017. URL: https://ec.europa.eu/clima/policies/transport/shipping_en.

[5] European commission. *communication from the commission to the european parliament, the european council, the council, the european economic and social committee and the committee of the regions the european green deal com/2019/640 final*. 2019. URL: https://eur-lex.europa.eu/legal-content/EN/TXT/?uri=COM$%5C%$3A2019$%5C%$3A640$%5C%$3AFIN.

[6] J Heywood. *Internal Combustion Engine Fundamentals*. New York, Verenigde Staten: McGraw-Hill Education, 2018.

[7] *IMO 2020 – cutting sulphur oxide emissions*. Dutch. 2020. URL: https://www.imo.org/en/MediaCentre/HotTopics/Pages/Sulphur-2020.aspx#:$%5C%7E:text=The%5C%20resulting%5C%20reduction%5C%20in%5C%20sulphur,respiratory%5C%2C%5C%20cardiovascular%5C%20and%5C%20lung%5C%20disease.$.

[8] IMO MEPC 72. *Initial strategy on greenhouse gas emissions from ship, Tech. rep. International Maritime Organisation*. Dutch. Apr. 2018.

[9] Ugur Kesgin. "Study on prediction of the effects of design and operating parameters on NOx emissions from a leanburn natural gas engine". In: *Energy Conversion and Management* 44.6 (Apr. 2003), pp. 907–921. DOI: 10.1016/s0196-8904(02)00093-6.

[10] MENENS. *Methanol als Energiestap Naar Emissieloze Nederlandse Scheepvaart*. Dutch. Aug. 2021.

[11] N.V. Nederlands Gasunie. *Basisgegevens aardgassen*. 1980.

[12] *Nitrogen Oxides (NOx) – Regulation 13*. Dutch. 2008. URL: https://www.imo.org/en/OurWork/Environment/Pages/Nitrogen-oxides-(NOx)-$%5C%E2%5C%80%5C%93-Regulation-13.aspx$.

[13] *Nitrogen oxides (NOx) emissions*. Aug. 19, 2010. URL: https://www.eea.europa.eu/data-and-maps/indicators/eea-32-nitrogen-oxides-nox-emissions-1/assessment.2010-08-19.0140149032-3.

[14] Roussopoulos. "A Convenient Technique for Determining Comparative Volumetric Efficiency". In: *SAE Technical Paper Series* (Feb. 1990). DOI: 10.4271/900352. URL: http://dx.doi.org/10.4271/900352.

[15] H Sapra et al. "Experimental and simulation-based investigations of marine diesel engine performance against static back pressure". Dutch. In: *Applied Energy* 204 (2017), pp. 78–92. DOI: 10.1016/j.apenergy.2017.06.111.

[16] H. Sapra et al. "Hydrogen-natural gas combustion in a marine lean-burn SI engine: A comparitive analysis of Seiliger and double Wiebe function-based zero–dimensional modelling". Dutch. In: *Energy Conversion and Management* 207 (2020), p. 112494. DOI: 10.1016/j.enconman.2020.112494.

[17] Z Schanger. *If shipping were a country, it would be the world's sixth-biggest greenhouse gas emitter*. Apr. 18, 2018. URL: https://www.weforum.org/agenda/2018/04/if-shipping-were-a-country-it-would-be-the-world-s-sixth-biggest-greenhouse-gas-emitter.

[18] T.W.P Smith, J.P Jalkanen, and B.A Anderson. *Third IMO Greenhouse Gas Study 2014*. Apr. 2014.

[19] D Stapersma. *Diesel Engines Volume 3 Combusiton*. Dutch. Faculty of Mechanical, Maritime and Materials Engineering - Delft University of Technology, 2010.

[20] Taylor. *The internal-combustion engine in theory and practice*. Revised. M.I.T. Press, Oct. 1985.

[21] S. Verhelst et al. “Methanol as a fuel for internal combustion engines”. Dutch. In: *Progress in Energy and Combustion Science* 70 (2019), pp. 43–88. DOI: 10.1016/j.pecs.2018.10.001.

[22] *Wärtsilä 32 Methanol Engine*. 2022. URL: https://www.wartsila.com/marine/products/engines-and-generating-sets/wartsila-32-methanol-engine.

[23] Z. Zhu et al. “Cylinder-to-cylinder variation of knock and effects of mixture formation on knock tendency for a heavy-duty spark ignition methanol engine”. Dutch. In: *Energy* 254 (2022), p. 124197. DOI: 10.1016/j.energy.2022.124197.